IEET
International Electrical Engineering Transactions

Vol. 5 No.1 (8)
January - June, 2019
ISSN 2465-4256

An online publication of the EEAAT
Electrical Engineering Academic Association (Thailand)
www.journal.eeaat.or.th

IEET – International Electrical Engineering Transactions

This journal is an online publication of the EEAAT, Electrical Engineering Academic Association (Thailand). IEET is published twice a year, ie., the first issue is for January – June and the second issue is for July – December.

EEAAT Journal Committee

IEET Editor

IEET (International Electrical Engineering Transactions) is published twice a year. Original contributions covering work in all aspects of electrical science, technology, engineering, and applications will be peer-reviewed by experts before publication. Topics of interest include the following: electrical power, electronics, telecommunication, control and system, sensor and measurement, optical technology, computer, information and communication technology (ICT), signal processing, social network tools and applications (apps), engineering education and other related fields.

For online submission of all manuscripts, correspondences, and letters, please visit
www.journal.eeaat.or.th

IEET Editorial Office

EEAAT - Electrical Engineering Academic Association (Thailand)
Room 409, F-Building,140 Cheum-Sampan Rd.
Nong Chok, Bangkok, Thailand 10530
Tel: +662-988-3655 ext 2216 Fax: +662-988-4026

IEET - International Electrical Engineering Transactions

Volume 5 (8)
Number 1
January – June 2019

PAPERS

Evaluation of the Effect of O_2-Ultra Fine Bubble on the Growth of Crustaceans

Ryota Ogaeri[1], Setsuko Koura[1]

[1]Chiba Institute of Technology/ Graduate School of Engineening
Chiba Institute of Technology / 2-17-1 Tsudanuma Narashino Chiba Japan
Tel.: +81-47-478-0418
E-Mail: s1523055UD@s.chibakoudai.jp

***Abstract*-Crustacea production is decreasing year by year. Ultra Fine Bubble water has characteristics showing a physiologically active effect on animals and plants. In this study, crayfish was used as an experimental individual and the influence of Ultra Fine Bubble water on the growth of the crustaceans was evaluated.**

Keywords-Ultra Fine Bubble, Crustacean, Crayfish, Moult, Dissolved oxygen

I. INTRODUCTION

Currently, food shortages are noted as a problem worldwide, and it is said about 850 million people are starving everyday earth. The world's population continues to grow, and is said to reach 9.6 billion in 2050. Therefore, we think that it is necessary to find new technologies in the field of aquaculture, agriculture, and livestock industry and to stable supply that is needed by consumers. Among them, we focused on the aquaculture field.

However, several problems have been identified in aquaculture. For example, raising a specific type of fish at high density has adverse effects not only on the tank used for the aquaculture but also on the surrounding environment. Specifically, by raising fish at a high density, feces discharged from the fish etc. are deposited under the tank. At the stage of decomposition of the aerobic by aerobic bacteria, oxygen is consumed and nondegradable organic matter is accumulated as sludge. In the summer, the concentration of oxygen near the bottom of the ocean where the organic matter in the deposited sediment is degraded by activated bacteria and greatly reduced. The poor oxygen water stirs the upper and lower sea water by strong winds, waves, and the sea surface cooling, and it is thought that this lowers the concentration of dissolved oxygen in the whole tank and causes a great obstacle to the fish. As described above, in the current aquaculture farms, there are problems such as deterioration of the water quality, respiratory disorders in the fish and breeding of germs due to poor oxygenation.

The technology that focuses on this concern is the Ultra Fine Bubble(Less than UFB). UFB are generally considered to be generated after the rapid contraction of micro bubbles as shown in Fig.1[1]. Since the bubbles are very fine, such as 1.0 μm or less, they are unique bubbles that can slowly rise and can be present in the water at high concentration for a long time. UFB is being researched in the fields of agriculture, fisheries and medicine. Growth promoting effects such as daikon radish and broccoli sprout have been reported in the agricultural sector by Oxygen Ultra Fine bubble water (Less than O_2-UFB)[2]. The Growth promotion effect of fish and removal of the norovirus from oysters have been reported.

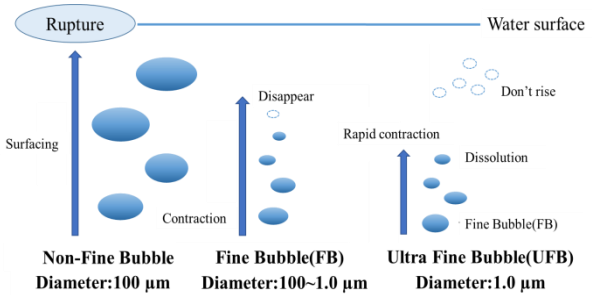

Fig. 1 Bubble commentary

Therefore, we used UFB water as breeding water and evaluated what kind of influence it has on the crustaceans. In the field of fishery, there have been some reports on fish research, but at the present there is no research on crustaceans. In the crustacean aquaculture, the growth rate and water quality are raised as problems. With regard to these problems, by using O_2 -UFB water, it is expected that the concentration of dissolved oxygen in the water can be increased to reduce the amount of the oxygen-deficient water mass, and that the growth promoting effect can be like that at fish. Furthermore, the amount of dissolved oxygen differs between the surface layer and the lower layer, and the amount of dissolved oxygen tends to be lower in the lower layer portion than in the surface layer. On the other hand, there are many types of crustaceans that inhabit the bottom[3],[4]. Therefore, we believe that a higher growth promotion effect can be expected for crustaceans by raising the amount of dissolved oxygen.

Therefore, in this study, we aimed to evaluate the effect of O_2-UFB water on crustaceans using the red crayfish, which is considered to be relatively robust and easy to observe its growth as an experimental individual.

II. PROCESS

2.1 Method of producing oxygen Ultra Fine Bubble

Using the compact UFB generator (Fig. 2), it was fabricated under the conditions listed in Table 1.

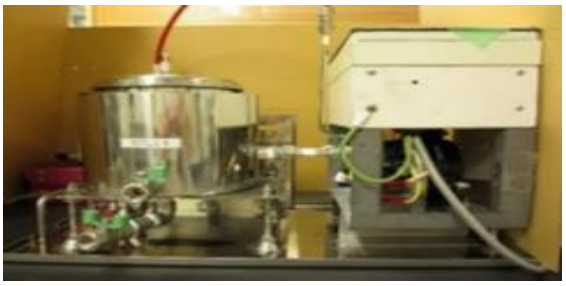

Fig.2 compact UFB generator

Table1 UEB water Production conditions

Tap water	1L
Gas species	O_2(purity99.99 %)
Rotation speed	4000 rpm
Time	10 min

2.2 Preparation mechanism of O_2-UFB

The generation schematic diagram of UFB by a gas-liquid mixing shear system is shown in Fig.3. The microbubbles generated by mixing gas and liquid from the IN side are sent to the ultrafine bubble generator at the pressure of the pump. The microbubbles are sheared by centrifugal force to generate the UFB.

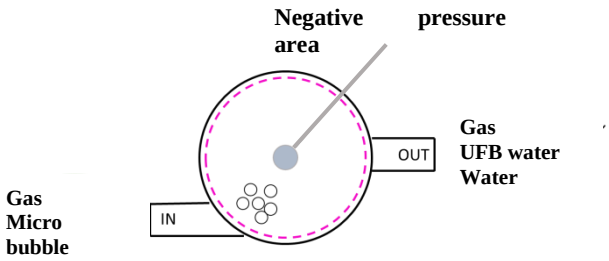

Fig. 3 Generation diagram of ultra-fine bubble by gas-liquid mixing shear method

2.3 How to cultivate the crayfish

A total of eight breeding tanks were (W17.5 cm × D11.3 cm × H11.0 cm) prepared, and 20 g of low floor was added to reduce stress on the crayfish and prevent molting failure. The amount of water was adjusted to 800 mL under two conditions of UFB water diluted twice with tap water (hereinafter-UFB 50%), and tap water (hereafter-tap water). Three tanks in which the crayfish was introduced and one tank in which the crayfish was not introduced were set up for each condition. The water temperature was kept in the range of 297.15 to 299.15 K during the breeding period. The frequency of water replacement was a half volume (400 mL) every other day, and the dissolved oxygen amount was adjusted to be about 20 ppm under the condition of UFB 50%. The experimental individuals emerged around April 2018. Six individuals with a length of 3.5 to 4.0 cm and a weight of 2.12 to 3.45 g were selected and used for the experiment. The frequency of feeding was set to continue eating artificial feed once every two days. The body weight of each individual was measured every other day, and the length was measured when they molted.

2.4 How to train the young crayfish

Fig.4 shows the rearing situation of the young crayfish. As experimental animals, individuals hatched around November 2018 were used, and 60 young crayfish were randomly collected. Thirty young crayfish were added under the to a water tank of 4.8 ℓ a two conditions of 50% UFB water and tap water, and reared for 10 days. The frequency of feeding was done0 every two days.

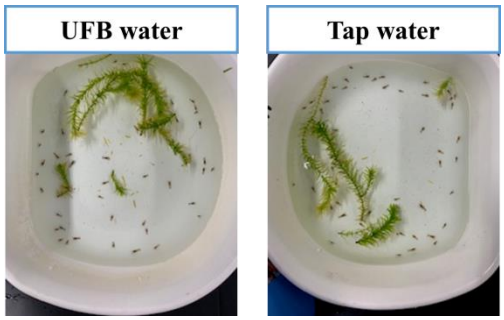

Fig.4 Breeding environment of young crayfish

2.5 Condition of each tank and how to begin

As individuals used for the experiment, 36 individuals having a length of 1.5 to 1.8 cm and a weight of 2.12 to 3.45 g were selected and used for the experiment. The tank was set up under the conditions of **Fig.5**. In the UFB tank, the dissolved oxygen content was adjusted to 20 ppm. We used a scale of (60 cm ×30 cm ×40 cm) in the aquarium and added gravel to prevent molting failure. Nine crayfish were added per condition, and the amount of water was 9.6 ℓ. The dissolved oxygen amount was adjusted to 20 to 22 mg / L in the tank of the UFB 50%, and the dissolved oxygen amount was adjusted to 6 to 8 mg / L in the tap water tank. The lighting was LED lights, the lighting time was 8 hours / day, and the water temperature was fixed at 298.15 K. during the breeding period. The frequency of feeding was once every two days, and the artificial feed was 10% of the body weight. The body weight of each individual was measured every other day, and the length was measured when molted.

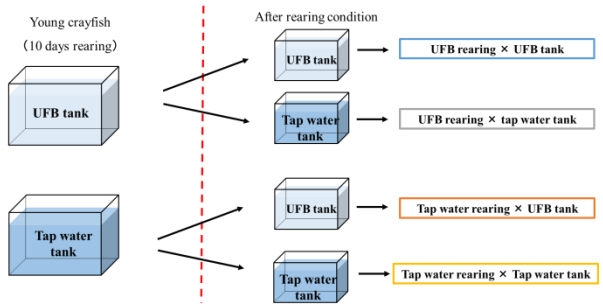

Fig.5 Experimental conditions

III. RESULTS AND DISCUSSION

3.1 Dissolved oxygen content and pH of tank under each condition

The time-dependent change in the amount of dissolved oxygen and pH of each condition is shown in **Fig.6**. The measurement was performed every hour after the water replacement for a total of 10 hours. Under the condition of UFB50%, it was confirmed that the dissolved oxygen amount after water replacement was 20-23 mg / L for both the crayfish and the blank. Under the condition without crayfish, the amount of dissolved oxygen decreases based on the sloping curve, and after 10 hours it becomes about 14 mg / L, Under the condition with the crayfish, it was confirmed that the amount of dissolved oxygen remarkably decreased after water replacement and decreased to 1 mg / L after 10 hours. Under tap water conditions, it was confirmed that the dissolved oxygen amount after water replacement was 7 to 8 mg / L with and without a crayfish, and the dissolved oxygen amount did not significantly change under either condition. It was confirmed that the amount of oxygen consumption is higher in the individuals grown under the condition of UFB50%. Based on these results, under the condition of UFB50% with the crayfish, the amount of predation and excretion becomes greater than that of a normal individual, the metabolism of the individual itself rises, and the water quality deteriorates and the microorganisms consume oxygen. Therefore, it was thought that the dissolved oxygen decreased.

Under the conditions of UFB50% and tap water, it was confirmed that the pH after water replacement was 7.7 to 8.1. Under the condition without crayfish, the pH did not significantly change. On the other hand, in the condition with the crayfish, the pH decreased with the passage of time for both the UFB 50% and tap water, and the tendency was more pronounced in the UFB 50% condition. This result was also confirmed for the dissolved oxygen, and it was also confirmed that the pH decreased as the dissolved oxygen decreased.

Based on these results, it was thought that the water quality deteriorated and pH decreased because the amount of predation and excretion increased more than for a normal individual under the conditions of UFB50% with the live crayfish.

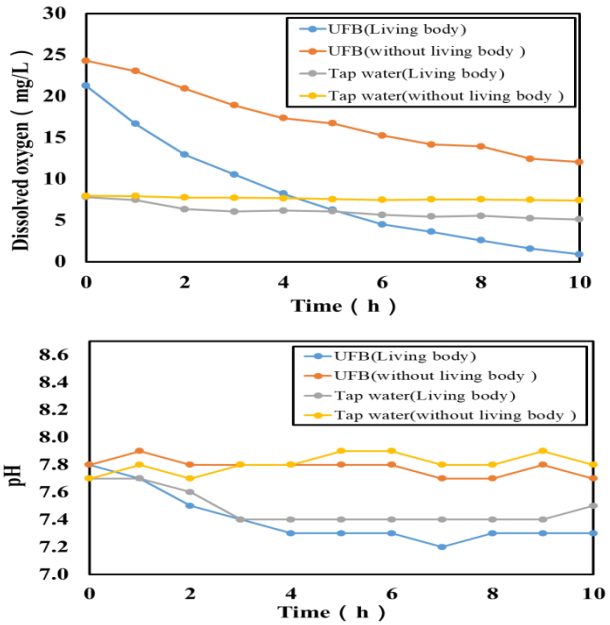

Fig.6 Relationship between dissolved oxygen content and pH change over time

3.2 Individual weight and length for each condition

The state of increase in body length when the crayfish molt is shown in Fig.7. As shown in Fig.7 when the conditions were compared, it was confirmed that the UFB 50% had a tendency to increase the length in proportion to the weight. Fig.7 shows the relationship between the time course of the crayfish and the weight. Since crustaceans generally change their weight significantly during molting, the red lines indicate areas where the weight was significantly changed by molting. The degree before and after molting is shown as a percentage. From the results shown in Fig.7, in the case of individuals reared under the UFB50%, condition a weight gain of 30% or more was confirmed when molted. On the other hand, only

an increase of about 20% was observed in individuals bred under the tap water conditions.

Under the tap water conditions, it is not possible to say in general because some individuals had not molted, but it has been confirmed that there is a large difference in the amount of feeding and oxygen consumption. This suggests that the O_2-UFB water has a positive effect on the crustacean growth.

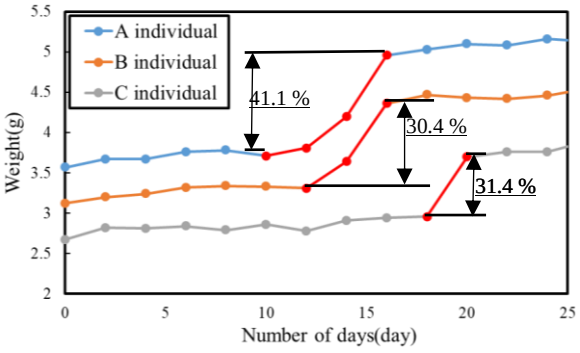

(UFB50%)

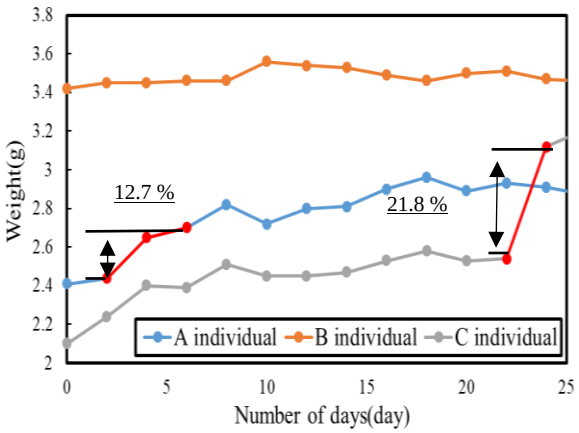

(Tap water)

Fig.7 Relationship between body weight of each individual and change over time

3.3 Average body weight, length and number of molting of young crayfish under each condition

Fig. 8 shows the relationship between average body weight and time course of each individual under each condition. It was confirmed that the average body weight of individuals under each condition was higher in the order of (UFB rearing × UFB tank) → (UFB rearing × tap water tank) → (Tap water rearing × UFB tank) → (Tap water rearing × Tap water tank). Based on the results, it was confirmed that the body weight increased when the water quality was changed, rather than rearing the crayfish in the same water.

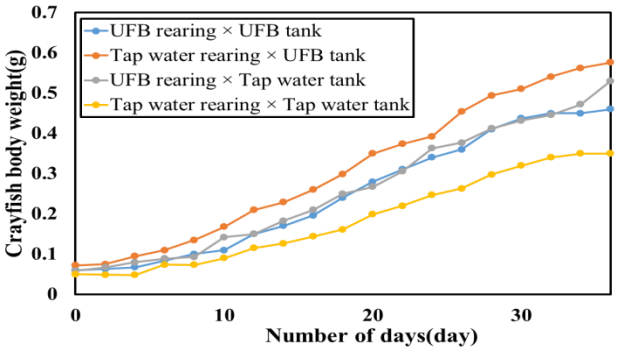

Fig.8 The average weight of each crayfish each condition

In Fig.9 for the change in body length due to molting of the crayfish is shown. It was suggested that the change in the body length is higher when the water quality changed as in the weight result.

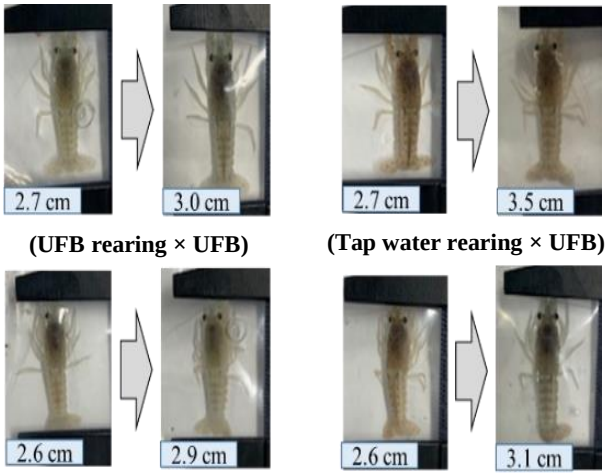

(UFB rearing × UFB) **(Tap water rearing × UFB)**

(Tap water rearing × UFB) **(Tap water rearing × Tap water)**

Fig.9 Changes in body weight due to molting of crayfish

Fig.10 shows the results of the number of molting times of each individual under each condition. Based on this graph, it was confirmed that individuals in the tap water tank varied from 1 to 6 times, while the number of molting times of individuals in the UFB aquarium increased from 4 to 6 times. From this, it was confirmed that the individuals grown in the tap water had variations in the number of molting times

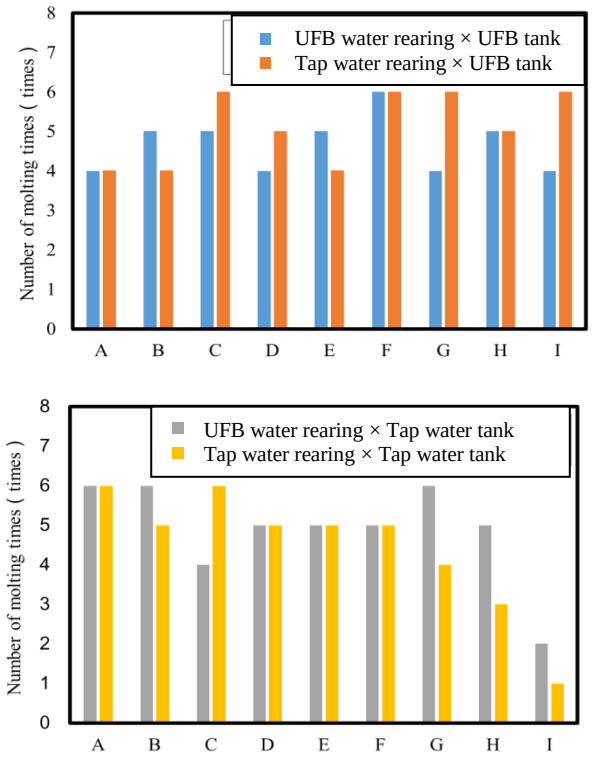

Fig.10 Number of molting times for each condition

In this study, we evaluated the effect of the O_2-UFB water on the crustaceans. First, regarding the water quality of the water tank, the DO and pH were measured. It was confirmed that the DO and pH of each condition tended to decrease in the water tank with individuals grown the UFB water. From this, it was thought that in the tank of an individual grown in the UFB water, the microorganisms consume oxygen by the increase of the amount of predation and the amount of excretion, and the water quality is lowered by decomposing the organic matter. In addition, it was also confirmed that the change in body weight due to molting was higher under the conditions of the UFB water tank even with the weight of the crayfish. It was confirmed that in addition to body weight, differences also occurred in length and predatory amount. From these facts, it was suggested that using UFB water as breeding water has a positive effect on crayfish. Therefore, we increased the conditions and rearing them from the young crayfish. As a result of measuring the body weight and the number of times of molting under a total of four conditions, it was confirmed that the average body weight was higher in the order of (UFB rearing × UFB tank) → (UFB rearing × tap water tank) → (Tap water rearing × UFB tank) → (Tap water rearing × Tap water tank). From this, it was confirmed that the average body weight tends to be higher if rearing the stage of the young crayfish under different conditions. Since differences in growth rates have been confirmed in crustaceans due to changes in water quality such as temperature and salinity in past studies, the stage of juvenile crayfish is similarly bred under different conditions in this study, and then by changing the environment, it was thought that a difference in the growth rate occurred [5].

IV. REFERENCES

[1] Tutomu Uchida, "Generation of micro- and nano-bubbles in water by dissociation of gas hydrates" *Korean Journal of Chemical Engineering IEEJ Journal of Industry Applications*, vol. 33, no. 5, pp. 1749-1753, 2016.

[2] Serina Endo. "Plasma & Micro/Nano Bubble(Fine bubble) to Agriculture and Aquaculture" *The 3rd International symposium on Application of High-voltage*, pp.83-84, 2018

[3] Katuyuki Hamasaki "Study on Reproduction and Development of Portunus trituberculatus" *Japan Society of Cultivation Fisheries Special Research Report*, 1996

[4] Johns D. M "I. Effect of temperature and salinity on survival, development rate and size, Marine Ecology-Progress Series" Physiological studies on Cancer irroratus lar-vae pp75-83, 1982

[5] Hiromichi Nagasawa "Crustacean hormone. Invertebrate hormones" Academic Publishing Center, 1998

The suppression effect of hydrogen fine bubble water on bacteria in water

Tomoyuki Matsumoto[1], Daichi Matsumaru[1], Yuriko Watanuki[1], Naoki Nemoto[1], Hitoshi Onodera[2], Koichi Hamaoka[2], Setsuko Koura[1]

[1]Chiba Institute of Technology / [2]Maxell Corporation / R&D Division
Graduate School of Engineering.
[2]Chiba Institute of Technology / 2-17-1 Tsudanuma, Narashino,
Chiba 275-0016, JAPAN
Tel.: +81-47-478-0418
E-Mail: s1523215SY@s.chibakoudai.jp

Abstract **Hydrogen fine bubble water, which can be easily produced by electrolysis, was used to evaluate the suppression effect on bacteria and slime. As a result of verification with the bacteria obtained from the remaining water in the bathtub, it was found that the hydrogen fine bubble water exerted a suppressive effect on some bacteria.**

Keywords— hydrogen fine bubble, bacteria, pink slime, Suppression effect.

I. INTRODUCTION

Pink stains may occur around a sink or tub containing water. This refers to a biofilm produced by microorganisms and is generally referred to as pink slime [1]. It is difficult to remove it. This is because bacteria exhibit a bactericidal resistance against drying, ultraviolet rays and chlorine by forming slime [2], [3],[4].

Fig. 1. Pink slimming that occurred in the sink.

To remove the slime, a periodic wiping and cleaning with ethanol and heat sterilization treatment ≧ 333.15 K is needed [5]. However, while these efforts are necessary, it is very difficult to continue.
Pink slime has a low toxicity. However, harmful black mold, etc., may multiply based on this [6].

Thus, it is currently required to suppress the formation of slime as a countermeasure.

Fine bubbles are bubbles of 100 to 1 μm size. Fine bubbles are known to have the effect of separating the hot bathing effect and dirt [7]. Among them, hydrogen fine bubbles have many advantages. The first point is that it is easy to make. They can be made by electrolyzing water, so it can be easily fabricated at home. As the hydrogen fine bubble water used in this study, a hydrogen generator for baths (H_2U manufactured by Maxell Co., Ltd.) was used to generate the hydrogen fine bubbles in tap water.

There is also the advantage that is no need to worry about chlorine itself or its toxicity due to by-products because it does not use a chlorine-based detergent for controlling the bacteria.

However, research on the bubble has been actively conducted, but the mechanism has not been elucidated yet [8].

Fig. 2. State of bubble generation.
(Source: Maxell Corporation Website)

In this study, I focused on the hydrogen fine bubble water generated by electrolyzing water. The inhibitory effect of the hydrogen fine bubble water on the bacteria and pink slime was investigated.

II. PROCESS

The composition of the standard agar medium used in this study was 2.5 g of yeast extract per liter, 5.0 g of peptone, 1.0 g of glucose and 15 g of agar. For the liquid medium solution, agar was omitted from this composition.

First, we identified the bacterial species in the bathroom and bathtub by a genetic analysis. Mucus and residual hot water collected from the bathtub and slime in the bathroom of the subject's house were spread on standard agar medium. They were then cultured at 303.15K. for 3 days to generate colonies. It was divided according to the color of the formed colony. Isolation and culture were carried out using a sterile toothpick. The isolation procedure was repeated three times. A partial sequence analysis of the 16srRNA gene was used for identification of the bacteria.

25 ml of liquid medium solution was weighed into a sterile Erlenmeyer flask. The bacteria were inoculated into this flask using a sterile toothpick and tilting the flask. It was cultured in a table-top shaking thermostat for 4 days at 303.15K.

An operation was performed to remove the liquid medium from the cultured bacterial solution. 1.0 ml of the cultured bacterial solution was collected in a sterilized 1.5 ml tube. The bacteria were precipitated using a centrifuge at 293.15K. and 8000 rpm for 3 minutes. The supernatant fluid (liquid medium solution) was removed by a micropipette and 1.0 ml of sterile water was added. This operation was repeated three times.

Next, the bacterial solution was serially diluted. After removing the liquid medium solution, it was diluted 10x, 100x, 1000x and 10000x with sterile water.

Finally, the diluted bacterial solution and various solutions were mixed 1: 1 and reacted for 1 hour.

The hydrogen fine bubble water used in this experiment is pure water or tap water and a hydrogen generator for the bath (H_2U manufactured by Maxell) placed in a plastic box, then 15 minutes elapsed after operation of the apparatus.

The inhibitory effect of the solution in this study was evaluated by a spot assay. The spot assay method is a method in which a small amount of the bacterial solution is spread on one standard agar medium. In this way, the bacterial solution prepared under many conditions can be evaluated on one agar medium.

Each 5 µl of the serially diluted bacterial solution was spread on a standard agar medium by a micropipette. After culturing for 4 days in a thermostat at 303.15K., the number of colonies was counted.

III. RESULTS AND DISCUSSION

As a result of culturing the pink slime and remaining hot water collected from the bathroom on a standard agar medium, colonies of with multiple colors as shown in Fig. 3 and Fig.4 were formed.

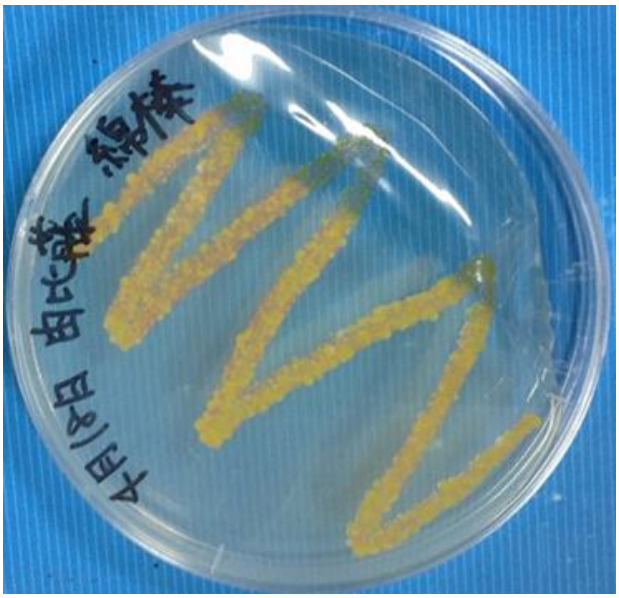

Fig. 3. Pink slime.

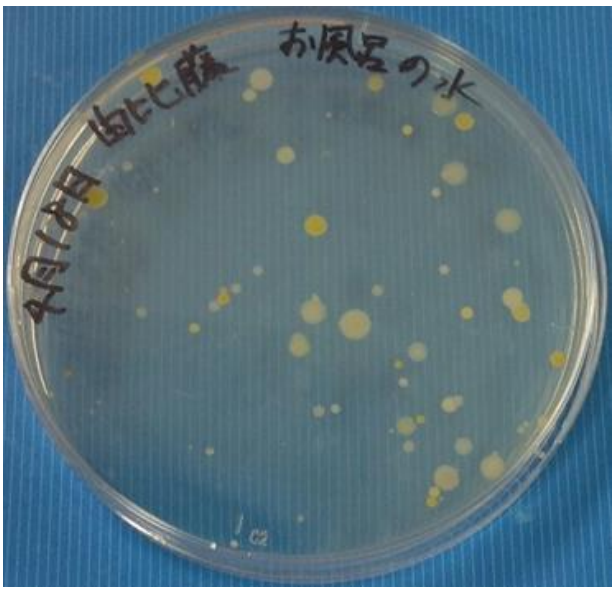

Fig. 4. Remaining hot water.

As a result of culturing the 16s rRNA partial gene after culturing the remaining hot water and slime in a standard agar medium, bacterial species as shown in Tables I and II were determined.

TABLE I

DETECTED BACTERIA (REMAINING HOT WATER)

Abbreviation	Name
Pink Bacteria	*Porphyrobacter* sp.
White Bacteria	*Enhydrobacter* sp.
Yellow bacteria	*Sphingomonas* sp.

TABLE II

DETECTED BACTERIA (SLIME)

Abbreviation	Name
Pink Bacteria	*Methyrobacterium* sp.
White Bacteria	*Brevibacterium* sp.
Yellow bacteria 1	*Sphingobium* sp.
Yellow bacteria 2	*Acidovorax* sp.
Orange bacteria	*Sphingomonas* sp.

From Table I, it was found that the pink slime contains not only pink bacteria but also of bacteria. In addition, it was found that there are different types of bacteria present in the remaining hot water and those present in the pink slime, and there are bacteria types which can be present in either species even if they are of the same genus or which appear with different colors to the naked eye.

Based on these results, it was found that a high number of detected bacteria was present in the water area, such as bacteria living in the water and bacteria forming slime.

It was necessary to determine whether the spot assay method, which is a comparative method, was suitable for this study. In general, comparison with plating was performed by plating the entire solution with an agar medium. Therefore, the serially diluted bacterial solution was plated and spot assayed to compare the number of colonies. The bacteria species examined here are the pink bacteria, white bacteria, and yellow bacteria collected from the remaining hot water. Furthermore, it was carried out using a total of 4 types of bacteria of common E. coli (MG1655) obtained from other laboratories.

TABLE IV

NUMBER OF COLONIES (PLATING)

Abbreviation	100x	1000x	10000x
Pink Bacteria	4040	668	138
White Bacteria	3264	448	62
Yellow Bacteria	2688	2152	736
E. COLI	4228	2004	282

TABLE III

Number of colonies (spot assay)

Abbreviation	100x	1000x	10000x
Pink Bacteria	256	33	4
White Bacteria	342	73	17
Yellow Bacteria	289	301	57
E. COLI	396	376	21

The amount of bacterial solution plated in the standard agar medium was 5 µl in the spot assay. 50 µl was used for the plating. Therefore, the formed colonies must be based on the above relationship.

Comparing the two tables, it is considered that a similar formation could be confirmed because the colony number shows some error but the total does not change.

It was then decided to incorporate a spot assay as a comparison method in this study.

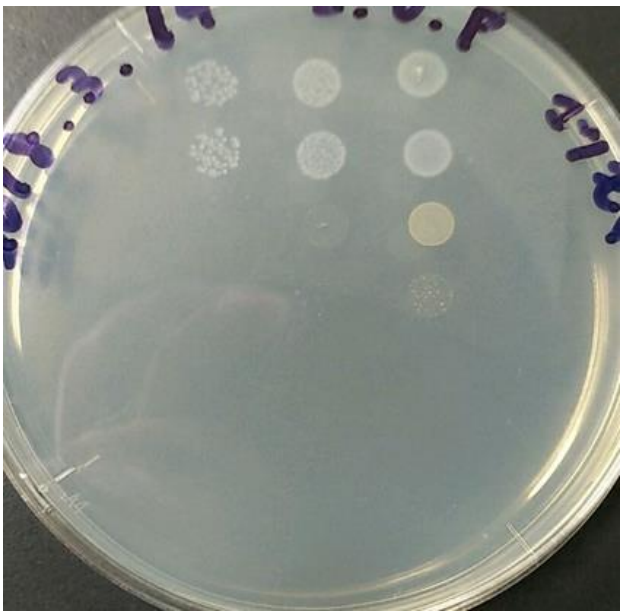

Fig. 5. Remaining hot water.

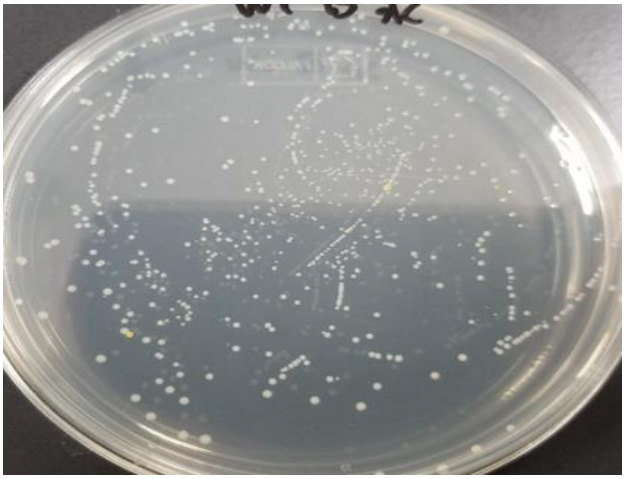

Fig. 6. Remaining hot water.

Next, we examined the suppression effect of the hydrogen fine bubble water. The bacterial species to be verified were the pink bacteria *Porphyrobacter* sp. (Hereinafter abbreviated as P) and white bacteria *Enhydrobacter* sp. (Hereinafter abbreviated as W), which were detected relatively frequently in the bacterial species collected from the remaining hot water.

First, it was determined how much the bacterial species P and W are affected by the chlorine contained in the tap water. Tap water generally used in the home contains 0.1 to 1 ppm of chlorine. The difference in colony formation was compared between sterile water (pure water) and tap water depending on the presence or absence of chlorine. Fig.7 shows the number of colonies of species W, and Fig.8 shows the number of colonies of species P.

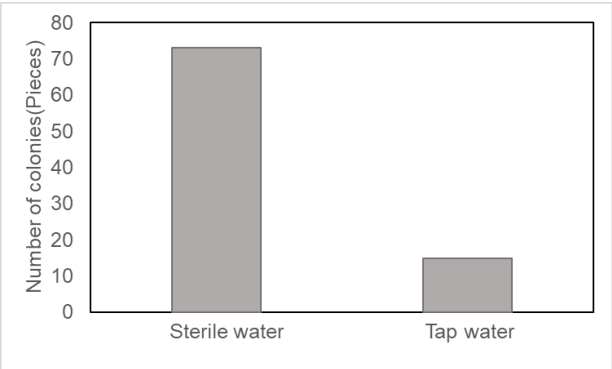

Fig. 7. The effect of chlorine (W)

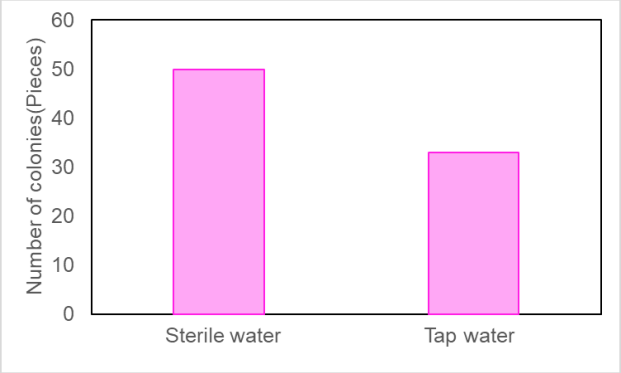

Fig. 8. The effect of chlorine (P)

As described above, it was found that both bacteria species are affected by the chlorine because the number of colonies in the tap water is low. In addition, since the number of colonies in the tap water is reduced to about 40% or less versus that of sterile water in the case of the bacterial species W, it is considered that chlorine is effective.

From the results, it was found that both the bacterial species P and the bacterial species W are affected by the chlorine. When making hydrogen fine bubble water with tap water, it is not known whether it is more effective than the bubbles or the effect of the chlorine. Therefore, it was necessary to make hydrogen fine bubble water with a solution which does not contain chlorine.

However, since the bath hydrogen generator used in this experiment is generated by the electrolysis of water, it was not possible to generate hydrogen fine bubbles with pure water. Therefore, bubbles were generated by adding sodium sulfate to the pure water. The reason for choosing sodium sulfate is that it is contained in ordinary tap water. Moreover, it is because it possibly does not have a big influence on the bacteria. The amount of sodium sulfate added was based on the standard amount established by the Water Supply Bureau of Narashino City, Chiba Prefecture, Japan.

Fig. 10. Pure water only.

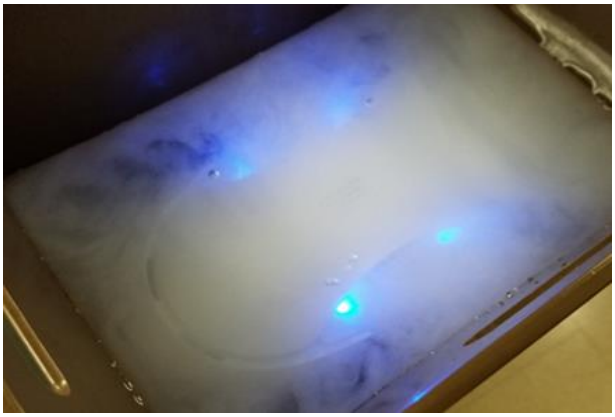

Fig. 9. Sodium sulfate added.

The comparison of the bacteria suppression effect of the various solutions was with sterile water, sodium sulfate added pure water (hereinafter referred to as modified water), tap water, hydrogen fine bubble water (modified water), and hydrogen fine bubble water (tap water).

Table V shows the number of colonies of the bacterial species W reacted with the various solutions. The number of colonies of the bacterial species P is also shown in Table VI.

TABLE V

NUMBER OF COLONIES (W)

Solution	100x	1000x	10000x
Sterile water	Many	44	10
Modified water	Many	49	2
Tap water	Many	5	0
H2 bubble water (modified water)	Many	58	3
H2 bubble water (Tap water)	Many	0	0

TABLE VI

NUMBER OF COLONIES (P)

Solution	100x	1000x	10000x
Sterile water	Many	68	12
Modified water	Many	56	5
Tap water	Many	46	6
H2 bubble water (modified water)	Many	58	3
H2 bubble water (Tap water)	89	4	0

First, with regard to the bacterial species W of Table V, a difference occurs between the tap water and modified water due to the influence of the chlorine. However, when the solution was used to make and add fine bubble water, the number of colonies significantly changed. Focusing only on the modified water, no change in the number of colonies was observed regardless of the presence or absence of the bubbles. On the other hand, in the tap water, the decrease in the number of colonies significantly changed. Producing hydrogen fine bubble water with tap water suppresses the bacterial colony formation more than tap water alone.

Based on these results, the effect of the hydrogen fine bubble itself on the bacterial species W could not be seen. However, it was found that hydrogen fine bubbles produced in the presence of chlorine suppressed the colony formation of the bacterial species W more than the ordinary tap water.

The same phenomenon was observed with the bacterial species P in Table VI. Although the amount of reduction was lower than that of the bacterial species W, the bacterial species P, which is highly resistant to chlorine, also had an inhibitory effect. It is thought that the hydrogen fine bubbles increased the suppression effect of chlorine. It is thought that safety can be enhanced if the bacteria can be suppressed with a lower concentration of chlorine than the normal tap water. It is necessary to elucidate this mechanism of action.

IV. CONCLUSIONS

In this study, we used hydrogen fine bubble water generated by the electrolysis of water to investigate the inhibitory effect on bacteria in the water.

First, as a result of identifying what kind of bacteria exist in the actual bathroom environment, pink bacteria, white bacteria and yellow bacteria were detected. Genetic analysis of them revealed that the pink bacteria were *Porphyrobacter* sp. and *Methylobacterium* sp. the white bacteria were *Enhydrobacter* sp. and *Brevibacterium* sp. and the yellow bacteria were *Shingomonas* sp. *Shingobium* sp. and *Acidovorax* sp.

The suppression effect by the hydrogen fine bubbles it was not seen against the white bacteria and pink bacteria detected from the remaining hot water. However, when it was done with tap water containing chlorine, it showed an inhibitory effect on the colony formation. It is possible that the hydrogen fine bubble increased the chlorine control effect.

REFERENCES

[1] Nozomu Ihara, Pink Monster Hiding in the Bathroom, Journal of the Society for Biotechnology, vol 94, p. 207, 2016.

[2] Katsunori Furuhata, Kazuko Koike, Atsuhiko Matsumoto, Behavior and chlorine resistance of Protomonas extorquens, which was frequently separated from the tank water for drinking, Journal of the Microbiology Society of Japan, vol 4, pp. 35-47, 1989.

[3] Katsunori Furuhata, Study on Chlorine-resistant Methylobacterium bacteria inhabiting tank water for drinks, 1995.

[4] Nobuo Shibata, Reversion of Housing and Life and Mold Contamination, Sanitation, vol 50, pp. 343-350, 2006.

[5] Yoshitoshi Ichiman, Kumi Asaga, Takahiro Ikeda, Kayo Kimura, Megumi Taketani, Changes in the Morphology and Viability of Ethanol for Disinfection, Changes in the Number of Viable Bacteria, Tsukuba Tech Junior Report, vol 6, pp. 269-272, 1999.

[6] Yoshihiro Arai, Industrialization of accelerating fine bubble technology, ARC report (RS-1007), 2016.

[7] Ashutosh Agarwal, Wun Jern Ng, Yu Liu, Principles and applications of microbubble and nanobubble technology for water treatment, Chemosphere, vol 84, pp. 1175-1180, 2011.

[8] Masaaki Morikawa, Let's examine the biofilm, Journal of the Society for Biotechnology, vol 90, pp. 246-248, 2012.

Influence of Inverter-Based Generation on Short Circuit Current Characteristics in Distribution Grids

Hafiz Iftikhar Ahmad, Wijarn Wangdee

The Sirindhorn International Thai-German Graduate School of Engineering (TGGS), KMUTNB
Bangkok, Thailand
hafiz.l-epe2016@tggs.kmutnb.ac.th, wijarn.w@tggs.kmutnb.ac.th

***Abstract*—This paper deals with the investigation of short-circuit current (SCC) characteristics in the presence of a high share of inverter-interface distributed generators (IIDGs) having dynamic grid support capability. The integration of renewable energy resources into distribution grids leads to an increased penetration with inverters as power sources. The fault current behaviour of inverters is different from synchronous generators. Characteristic values of the SCC play an important role in the design/dimensioning of equipment and protection systems for grid planning. Therefore, different fault scenarios in a benchmark medium voltage grid are simulated to analyze the impact of IIDGs on SCC behaviour. To model the inverter fault current behaviour, a generic model for Photovoltaic (PV) power plants is used. The results for simulated scenarios show that the SCC behaviour is influenced by the controller response at the high share of IIDG.**

Keywords—Dynamic grid support; inverter-interface distributed generator (IIDG); short-circuit current

V. INTRODUCTION

The electrical power system is evolving in terms of structure and technology. In Germany, this transition is prominent due to the Federal Government's Energiewende project, which sets a target to shut down the nuclear and coal-based power plants by the year 2022 [1]. On the other hand, decentralized energy resources (DERs) have increased rapidly in recent years and still growing to meet energy consumption [2]. These objectives are changing the power system significantly and continuously in terms of operation and structure.

The increasing share of DERs, primarily PV power plants connected to the grid through the power electronics converters commonly known as inverter-based generators or inverter-interface distributed generators (IIDGs), have put forth many challenges. These challenges include instability for the power distribution authority as a result of the sudden disconnection of IIDGs during the grid faults. The German national grid code for IIDG is modified to provide low voltage ride-through (LVRT) capability to support grid voltage dynamically by injecting reactive current during the fault depending on the generator type and voltage level [3]. However, another subsequent problem appeared because of the fault current being delivered by IIDG into the grid during the faults due to the fast response of inverter control.

According to the standard IEC-60909, fault current characteristics are described by either the fault is near or far from the synchronous generator. Both cases are based on the modelling of power grid as a common voltage source with equivalent internal impedance. Due to the mentioned changes in the power system, the fault current characteristics might also change in the future. Therefore, the investigation is carried out in this paper to study the SCC behaviour in the presence of a high share of IIDG.

DIgSILENT PowerFactory, a widely used power system analysis software, is utilized to perform the SCC simulation. The electromagnetic transient (EMT) simulation function in DIgSILENT PowerFactory is used to obtain the instantaneous SCC behaviour. To analyze the impact of IIDG on SCC, WECC generic model defined for the large-scale PV plants [4] is used as a plant level controller at the point of interconnection. The WECC model is suitable for transient and voltage stability studies. The controller model is adjusted to provide the reactive current injection at the voltage dips respecting to the grid code. In this paper, the scenarios regarding the increasing share of IIDGs are studied under the symmetrical faults in the power network.

The paper is organized as follows. The theoretical background regarding SCC calculation, German grid code and WECC PV model is described in Section II. Methodology and study system to proceed further is presented in Section III. Finally, the results and conclusion are illustrated in Sections IV and V, respectively.

VI. THEORETICAL BACKGROUND

In a conventional power system, energy is transferred from large generating units to load centres through the transmission and distribution grids. This system is characterized by uni-directional power flow from higher to lower voltage levels. But due to a massive integration of (DERs), power plants of various sizes exist at all voltage levels. In contrast to the conventional power system, modern grids can have a bi-directional power flow. This development makes the power system more complex in terms of operation and design [5]. The performance of the electrical power system is required to investigate and make the operation safe and reliable. The

short-circuit study is one of the basic studies executed to know the maximum and minimum fault current flows during the fault. This paper focuses on the maximum fault current that is required to define the withstand capability of the electrical equipment (i.e. cable, transformer, circuit-breaker) [6].

Short-Circuit Current (IEC-60909)

The standard IEC-60909 is used to calculate SCC in the three-phase AC system as less detailed grid information is required. This standard is also adopted as German standard named as VDE-0102. This standard defines two types of SCC characteristics depending on the fault location from the generation point. In case of fault far-away from the synchronous generator, it is assumed that AC-component of fault current remains constant. Whereas, the fault close to a synchronous generator is considered having decaying AC-component [7]. The SCC characteristics associated with a fault far from and close to the generator [8], respectively, are illustrated in Fig. 1 and Fig. 2.

Where:

I″k initial SCC
ip peak SCC
Ik steady-state SCC
A initial value of DC-component

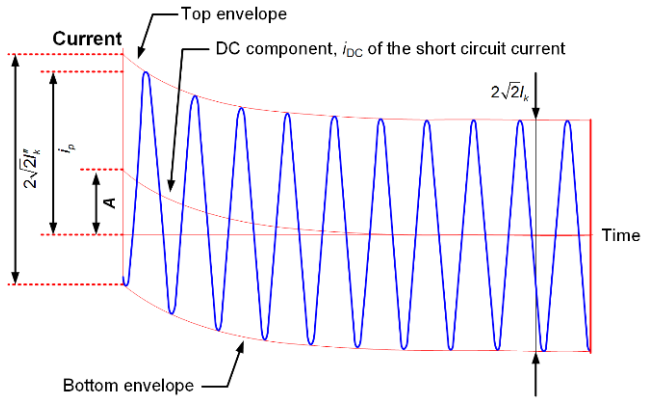

Fig. 1 SCC Characteristics for a Fault Far-away from the Synchronous Generator

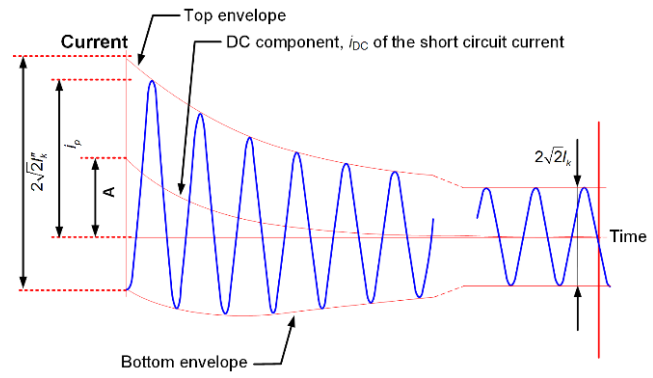

Fig. 2 SCC Characteristics for a Fault Close to the Synchronous Generator

I″kmax is the initial value of the SCC which is also known as the sub-transient SCC. The steady-state SCC *Ik* for the fault far-away from the synchronous generator is assumed to be equal to the sub-transient SCC respecting to the standard. But the sub-transient SCC is different from the steady-state SCC for a fault occurred close to a synchronous generator. The maximum sub-transient SCC flows in the power grid only when the fault occurs at zero crossing of the voltage waveform.

The DC-component is the decaying component in both types of SCC characteristics. The decay rate of the DC-component depends on the instantaneous value of the voltage at the time of fault occurs and the power factor of the system at the fault point [9].

The SCC calculation according to the standard is based on the calculation of internal impedances and a common voltage source. All the line capacitances and admittances of non-rotating loads are assumed to be neglected. The full power converter generator (inverter-based generation) such as photovoltaic is represented as a simple current source for maximum short-circuit current contribution during a fault. The impedance of each equipment must be referred to the voltage level of the fault point [10]. The impedance of all the power grid equipment can be calculated by the formulas given in VDE-0102 [7].

German Grid Code

The guideline for IIDGs integrated into the medium voltage grid [3] is modified to provide the dynamic grid support for grid faults creating voltage dips at the point of common coupling (PCC).

Regarding the guideline defined in [3], each IIDG should have the ability to stay connected during the voltage dips which is described in the low voltage ride-through (LVRT) curve as shown in Fig. 3. In zone A, IIDG should remain connected to support the voltage. The connection of IIDG and reactive current injection in zone B is required to help the system voltage in accordance with the agreement with the distribution grid operator. In zone C, instant disconnection of IIDG is accepted.

The dynamic voltage support capability defines the reactive current from IIDG based on the voltage at PCC. According to the guideline [11], it is not allowed to inject reactive current to influence the voltage within the ±10% of voltage variation to improve the system stability. The reactive current injection is defined by the slope of the line shown in Fig. 4 [11] which depends on the factor *k* shown in the equation below. The slope factor *k = 2* is used in this research study to inject the reactive current equal to the rated current of the inverter at the voltage equal to 0.5 pu. The control response time of reactive current injection should be less than 20 ms.

$$k = (\Delta IB / IN) / (\Delta U / UN) \geq 2.0\ pu$$

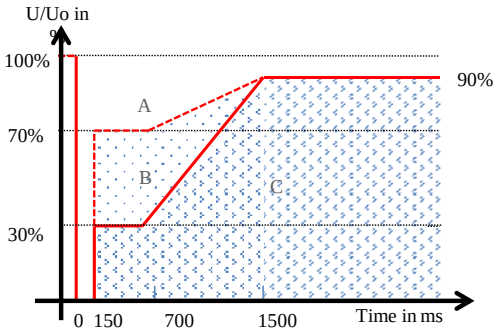

Fig. 3 LVRT Guideline for IIDG Connected at Medium [3]

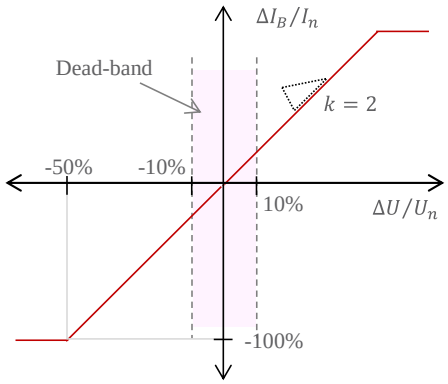

Fig. 4 Reactive Current Injection Requirements for Voltage Support [11]

WECC Generic PV System Model

The generic PV system model is defined to provide a good representation of the dynamic electrical performance of photovoltaic power plants at PCC with the large power system. The model is suitable to study the system response for electrical disturbances outside the PV power plants, not for the solar irradiance transients (solar power is assumed constant over the simulation period) [12]. The overall model structure of large-scale PV plants defined by WECC [4] as shown in Fig. 5. It can be seen that the model is divided into three parts;

- Renewable Energy Generator/Converter (REGC_A): sets up current injection within limits.
- Renewable Energy Electrical Control (REEC_B): generates active and reactive current references.
- Renewable Energy Plant Control (REPC_A): is for active and reactive power control at the plant level.

The REGC_A is required to run the simulation regardless of control mode while using the WECC generic PV system model [12]. However, the control mode can be defined regarding the functionality requirement through REEC_B and REPC_A. The REEC_B is necessary for this study as it provides control attributes for dynamic grid support. On the other hand, REPC_A is an optional module, which is not used in this paper and the model is initialized from solved power flow parameters.

1) REGC_A Model

The REGC_A model consists of a high bandwidth current regulator which is directly interfaced with generator model and injects reference current *Id_ref* and *Iq_ref*. The structure of REGC_A model [4] is described in Fig. 6.
The high voltage reactive current management (HVRCM) allows reactive current control during high voltage events. The current command remains the same as that generated in REEC_B for the low voltage events. Active current management is required to control the response of the inverter during the voltage dips in order to imitate the inverter phase-locked loop (PLL). Power logic generates a controlled response of active current following the voltage dips.

2) REEC_B Model

The REEC_B model [4] is shown in Fig. 7 and its functional structure is briefly explained below.

REEC_B_1: fault ride-through offers reactive current injection to control the terminal voltage by calculating the voltage dip.

REEC_B_2: the values *Qinitial* and *Pinitial* are calculated from the power flow solution. It offers different control modes to regulate the voltage at PCC by controlling the power factor and reactive power as explained in [4]. Constant Q control is selected with respect to the scope of the paper.

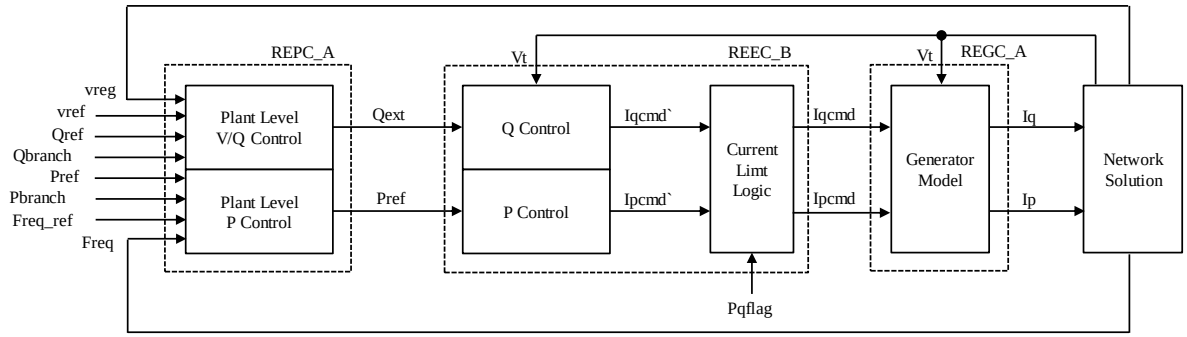

Fig. 5 Overview of WECC Dynamic Model for PV Plant [4]

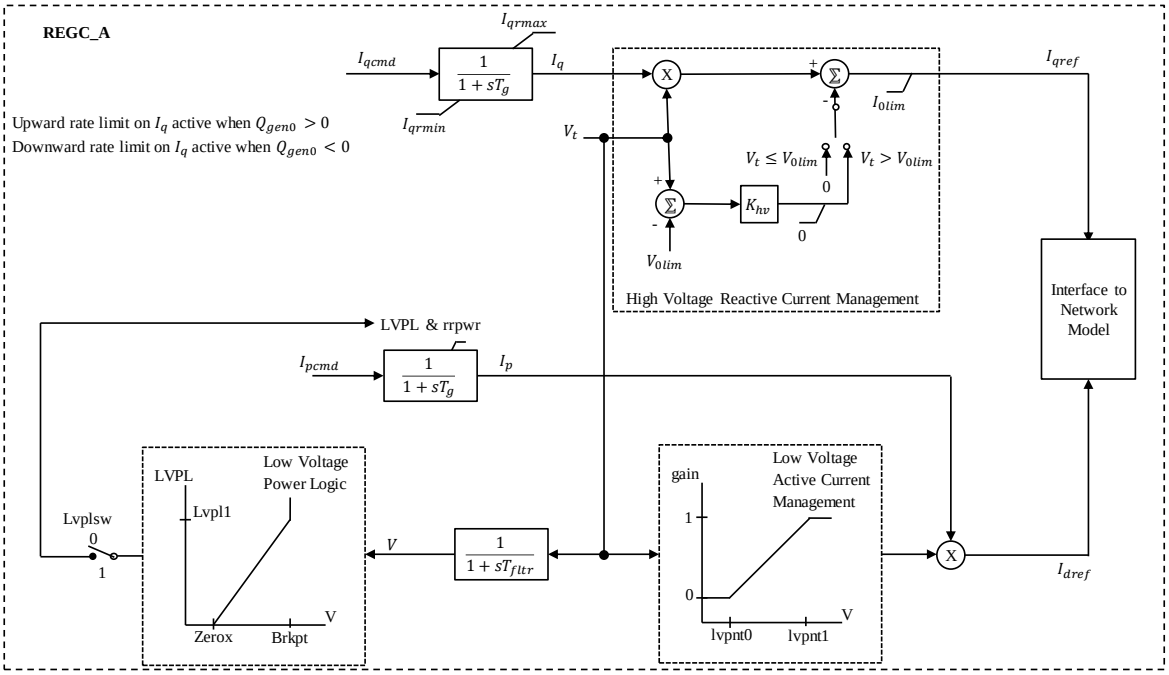

Fig. 6 Block Diagram of REGC_A [4]

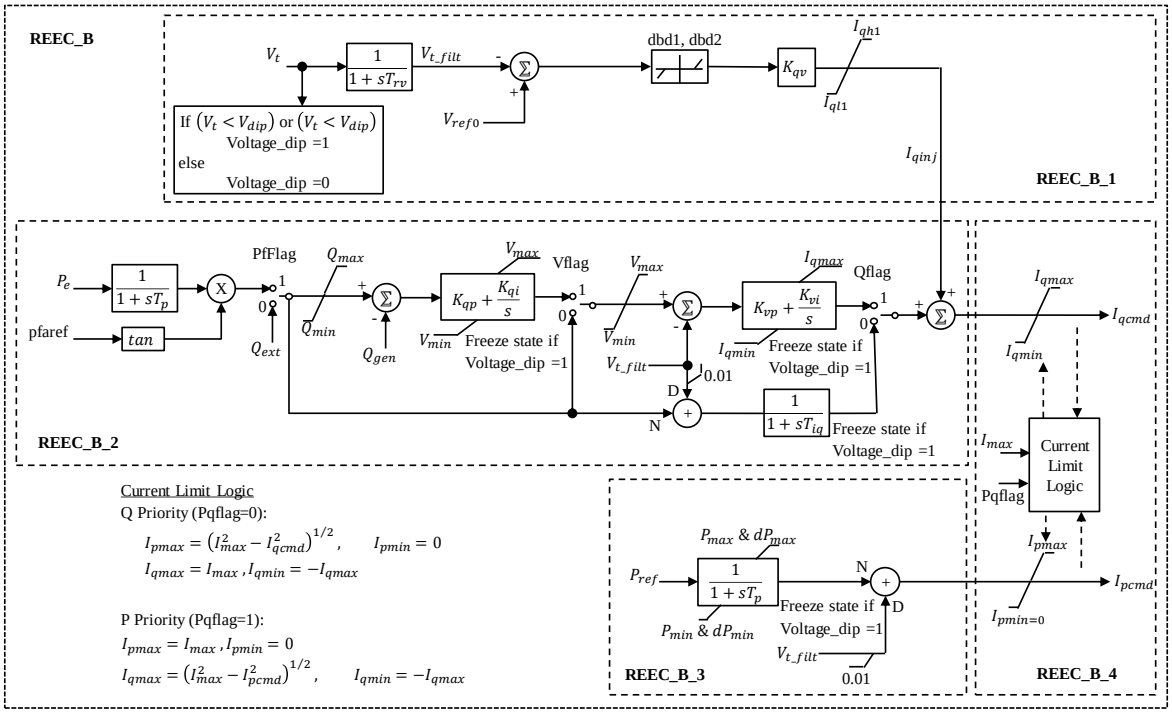

Fig. 7 Block Diagram of REEC_B [4]

REEC_B_3: P control provides the active current command respect to the filtered voltage and reference active power determined in the grid solution which is limited by ramp rate limits and power limits.

REEC_B_4: current limit logic provides the maximum and minimum limits of active and reactive current command (*Ipcmd*, *Iqcmd*) explained by the equations shown in Fig. 7. The reactive current injection is subject to the user-selectable priority between active and reactive current by selecting the priority flag *(Pqflag)*. *Pqflag = 0* is selected to prioritize the reactive current command over active current command for the voltage dips required to follow the grid code.

VII. METHODOLOGY AND STUDY SYSTEM

This section describes the general method and implementation procedure to complete the goal of the paper. To perform SCC calculation in the distribution grid, European version of the CIGRE medium voltage benchmark grid [13] is selected as a reference grid shown in Error! Reference source not found.. The MV grid is a three-phase system at a frequency of 50 Hz and a nominal voltage of 20 kV. The parameters of each equipment used in this analysis are same as given in the CIGRE documentation [13]. The 1000 MVA is used as an MVA short-circuit rating of MV grid feeder. The dynamic behaviour of load is not considered in this study to avoid further complications with the system dynamics. The load at bus-6 (circled) in the MV grid is extended with MV/LV transformer and LV load as shown in Error! Reference source not found..

In order to inspect the SCC behaviour, the selected approach is explained in Fig. 9. An ideal three-phase fault is simulated in this paper because it develops a maximum fault current in most of the cases respecting to the standard. The instantaneous fault current behaviour in the distribution grid is analysed and compared with the presence and absence of the PV plant.

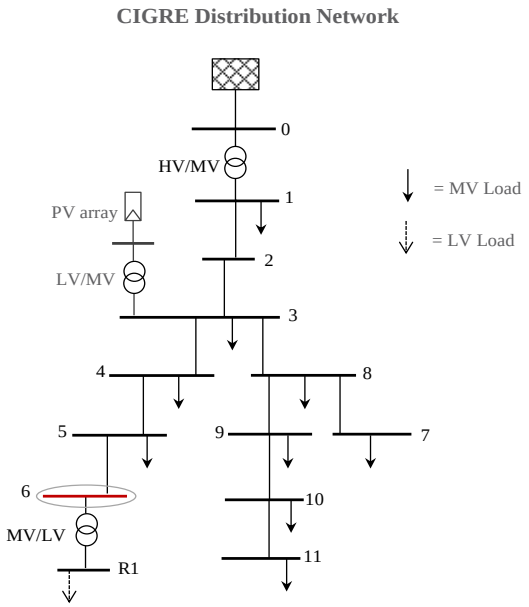

Fig. 8 Reference Distribution Grid (CIGRE) [13]

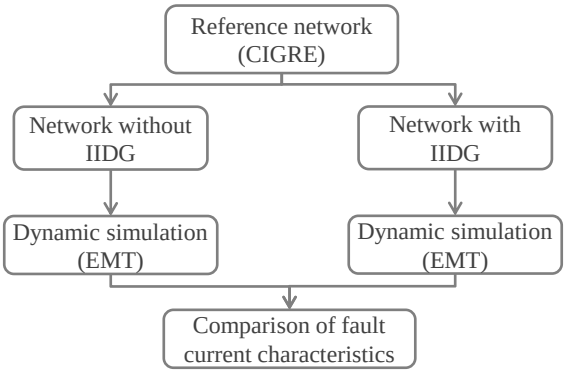

Fig. 9 Fault Current Investigation Approach

One aggregated large–scale PV plant connected at bus-3 of MV grid shown in Fig. 8 is considered in this paper instead of using many small PV plants by assuming the similar controller response time for reactive current injection. The response time of 19 ms is used in this paper. The WECC generic model for PV plant is modelled as a current controlled voltage source. The modified parameters of the WECC model are listed in TABLE I.

The fault current of the system associated with the three different penetration levels of PV plant is investigated to analyse the influence of reactive current injection on the SCC characteristics. These three PV plant sizes to be installed at bus-3 (one size at the time) is described in TABLE II.

TABLE I. MODIFIED PARAMETERS OF WECC MODEL

Description	Symbol	Value
Maximum apparent current (pu on mbase)	*Imax*	1
Maximum reactive current injection (pu on mbase)	*Iqh1*	1
Minimum reactive current injection (pu on mbase)	*Iql1*	-1
Overvoltage deadband for reactive current injection (pu)	*dbd1*	-0.1
Undervoltage deadband for reactive current injection (pu)	*dbd2*	0.1
Reactive current injection gain (pu/pu)	*Kqv*	2
Low voltage condition trigger voltage (pu)	*Vdip*	0.9
Enable (1) or disable (0) low voltage power logic	*Lvplsw*	0

TABLE II. SIMULATED RATINGS OF PV PLANTS

Study Scenario	Case_1	Case_2	Case_3
PV Plant size (MVA)	3	6	15

IV. STUDY RESULTS

The investigation of SCC characteristics is conducted based on two fault scenarios; the first scenario is by applying the three-phase fault to MV grid at bus-6, and the second scenario is by applying the three-phase fault at LV bus-R1. In both scenarios, the SCC characteristics with and without the PV plant are compared as shown below.

A. SSC Characteristics due to Fault in MV-bus

In this fault scenario, a fault is applied at bus-6 of the MV grid. The instantaneous SCC for the complete grid without PV plant is shown in Fig. 10. As expected, the SCC characteristic shown in Fig. 10 is similar to the SCC characteristic of the fault far away from the synchronous generator as previously illustrated in Fig. 1.

For benchmarking purpose, Fig. 10 is used as a reference to compare against the SCC characteristics of the grid when the PV plant is installed at bus-3, which is illustrated in Fig. 11 to Fig. 13 for Case_1 to Case_3, respectively.

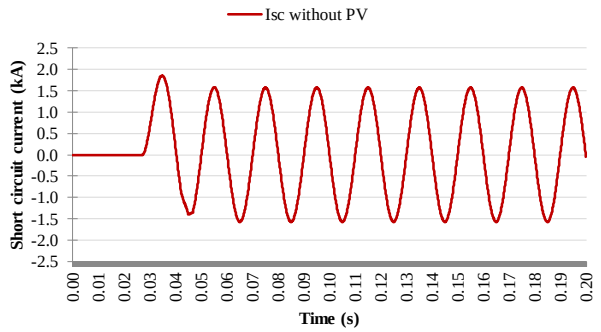

Fig. 8 Isc for Fault at Bus-6

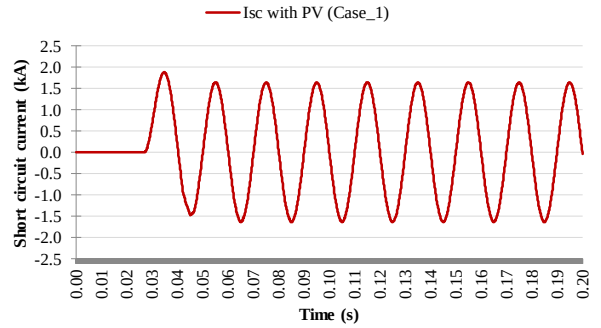

Fig. 9 Isc for Fault at Bus-6 (Case_1)

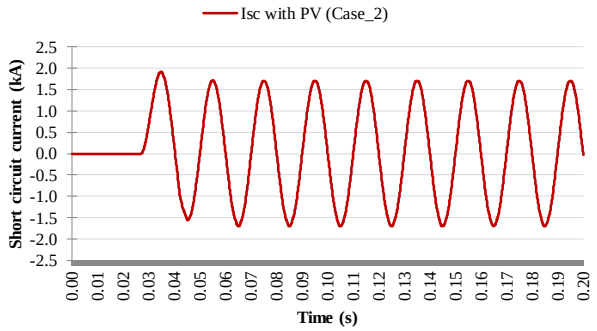

Fig. 10 Isc for Fault at Bus-6 (Case_2)

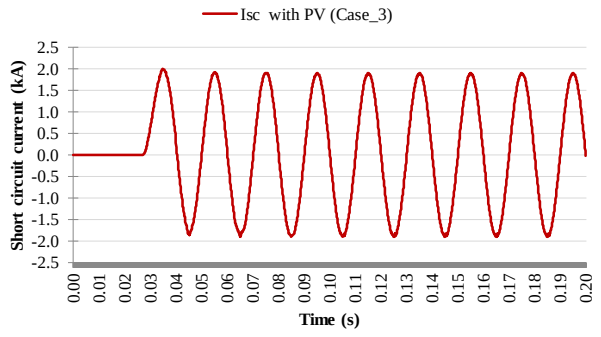

Fig. 11 Isc for Fault at Bus-6 (Case_3)

It can be observed from Fig. 11 to Fig. 13 that the magnitude of the short-circuit current (Isc) increases as the size of the installed solar PV plant increases. When the low amount of the PV plant (i.e. with 3 MVA in Case_1) is installed, the SCC characteristic is relatively similar to the reference shown in Fig. 10 (i.e. without PV installed). However, as the size of the installed PV plant is increased, the first cycle instantaneous SCC peak becomes relatively close in magnitude compared to the second cycle peak as shown in Fig. 13 for Case_3 (i.e.15 MVA). This SCC characteristic is fundamentally different from the benchmarked SCC characteristic shown in Fig. 10. Furthermore, it is not possible to observe SCC characteristic with the large size of PV plant as short circuit ratio (SCR) at PCC become less than the operating limit of WECC generic model. The generic model for PV plant developed by WECC is only applicable for systems having SCR $\geq$ 3 at PCC [4]. The SCR for case_3 is equal to 3.49 which is close to the operating limit of WECC generic model.

The results shown in Fig. 10 to Fig. 13 are depicted altogether as presented in Fig. 14 for a comparison purpose. It can be clearly seen in Fig. 14 that the SCC characteristics associated with Case_3 (i.e. 15 MVA PV plant) behaves differently compared to the cases with a lower amount of PV installations. Therefore, it is interesting to further investigate the altering SCC behaviour. The phase voltage and reactive current injection from the 15 MVA PV plant at bus-3 (Case_3) during the fault at bus-6 are plotted as shown in Fig. 15 and Fig. 16.

It can be observed from Fig. 15 that when the fault occurred at bus-6, the voltage at bus-3 (i.e. PV installed bus) drops below 0.4 p.u. This is because bus-3 is electrically close (in distance) to bus-6 where the fault occurred. Thus, this very low voltage condition at bus-3 results in the reactive current injection at maximum (100%) capacity of the PV inverter as shown in Fig. 16. When the size of the PV plant is considerably large (i.e. 15 MVA in Case_3), then the reactive current injection at its maximum capacity becomes significant on the SCC characteristic in this case. On the other hand, when the size of PV plant is not large (i.e. 3 MVA in Case_1 and 6 MVA in Case_2), the reactive current injection from the PV controller is not enough to alter the SCC characteristics prominently. Therefore, the SCC characteristics are still similar

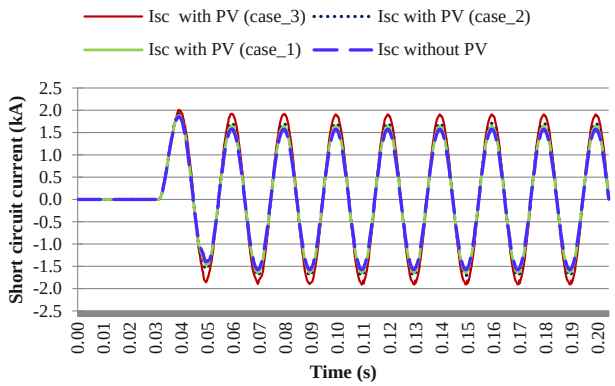

Fig. 12 Comparison of Isc for Fault at Bus-6

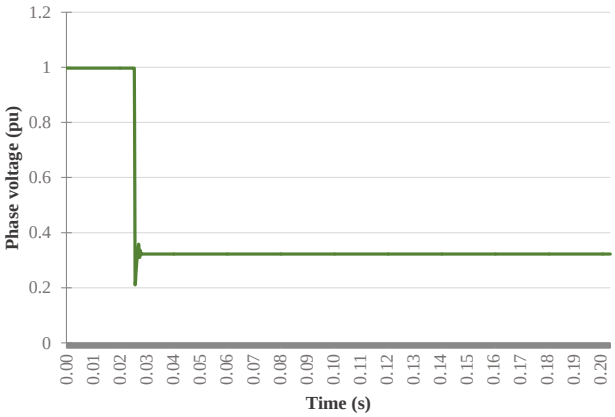

Fig. 13 Phase Voltage at the PV Installed Bus for Fault at Bus-6 (Case_4)

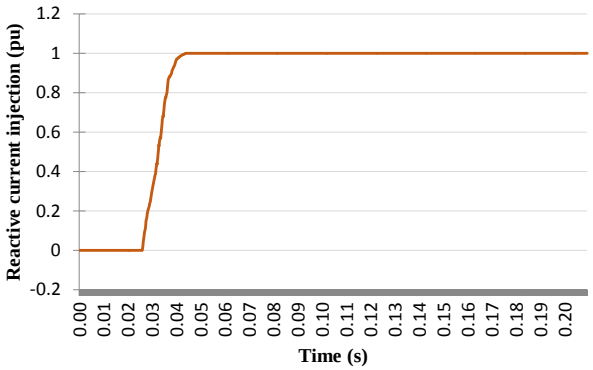

Fig. 14 Reactive Current Injection by PV Controller for Fault at Bus-6 (Case_4)

to that of a synchronous generator as previously illustrated in Fig. 9 and Fig. 10.

B. SCC Characteristics due to Fault in MV-bus

In this scenario, the short circuit is applied to LV bus-R1 shown in Fig. 8, while the installed PV plant is still connected to bus-3 (i.e. on the MV grid). Fig. 17 presents the SCC characteristic comparison for the system without and with the PV plant installed. It can be seen from Fig. 17 that the peak value of the fault current (at the first half cycle) without the PV plant installed yields the lowest value, whereas Case_3 (i.e. 15 MVA PV plant) results in the highest peak value the fault current.

It is worth noting that the SCC characteristic associated with Case_3 during the fault at the LV bus is similar to the fault far away from the synchronous generator in which the highest peak value of the fault current taken place in the first half cycle. This conclusion is opposite to the scenario presented in the previous sub-section when the fault occurred at the MV bus, where Case_3 produces the highest peak value of the fault current and the second half cycle peak is very close to peak of the first half cycle. It is therefore interesting to further investigate the phase voltage and reactive current injection from the 15 MVA PV plant at bus-3 (Case_3) during the fault at bus-R1 are plotted as shown in Fig. 16 and Fig. 17.

Fig. 16 indicates that the phase voltage dip at the PV plant (bus-3) during the fault at bus-R1 is not much, i.e. around 0.89 pu after the fault. This small voltage dip is due to the fact that the fault occurred at the LV grid (bus-R1) where it is electrically quite far away in distance to the PV plant location (bus-3). This, voltage dip is not low enough to produce a maximum (100%) reactive current injection at its rated capacity of the PV controller as shown in Fig. 17.

The reactive current injection from the 15 MVA solar PV plant shown in Fig. 17 is around 0.21 pu of its rated capacity in this case. This 0.21 pu reactive current injection is not enough to get a significant shift in the SCC characteristic at the second half cycle during the fault, and therefore the SCC characteristic associated with Case_3 remains similar to that of the fault far away from the synchronous generator.

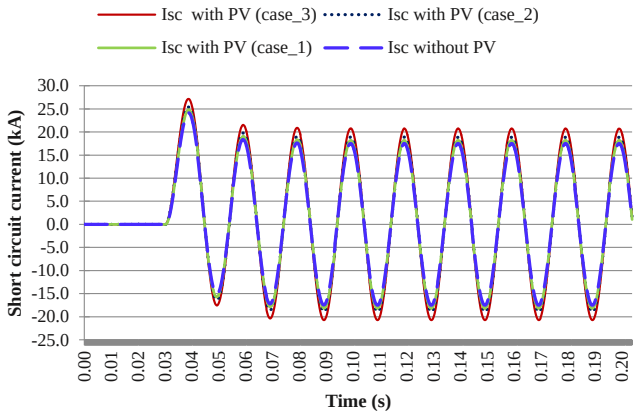

Fig. 15 Comparison of Isc for Fault at Bus-R1

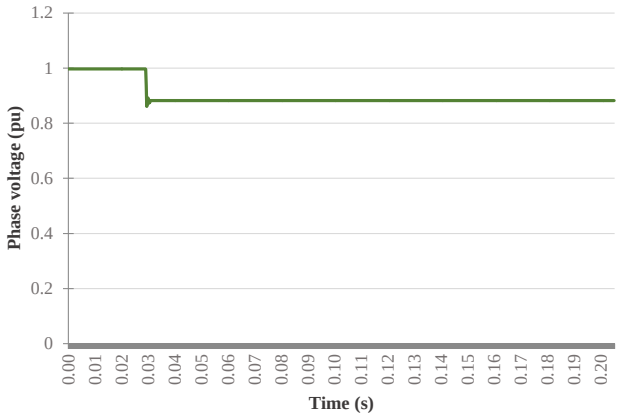

Fig. 16 Phase Voltage at PV Installed Bus for Fault at Bus-R1 (Case_4)

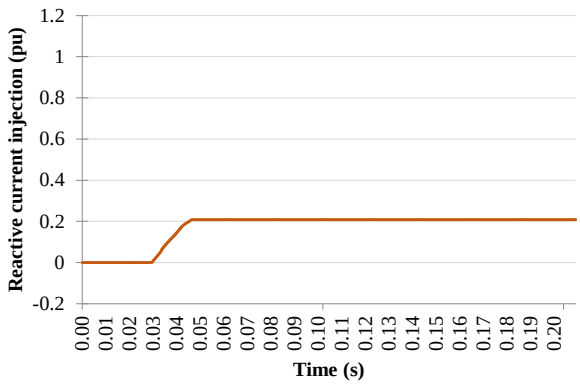

Fig. 17 Reactive Current Injection by PV Controller for fault at Bus-R1 (Case_4)

VIII. Conclusions

In this research work, the influence of IIDG having dynamic grid support on SCC characteristics is studied necessary to define the correct withstand capability and protection settings of the equipment. Regarding the simulated results, it can be concluded that SCC behaviour is changed in the presence of a high share of IIDG in the MV grid when the fault occurred electrically close to the large-scale PV plant. The change in SCC is dominated by the PV controller response time and SCC peak still occurs in the first half cycle as traditionally but very close to the peak of the second half cycle which is not similar to the classic representation.

There is a scope to use detailed vendor-specific models instead of generic models to analyse SCC characteristics with bigger PV plants than used in this paper. In future, it is also possible to use controller with faster response time than used in this paper to provide a thorough investigation. The behaviour of the fault current can also be studied with weaker grids and complex networks including load dynamics.

IX. References

[1] Agora Energiewende, Projected EEG Costs up to 2035: Impact of expanding Renewable Energy According to the Long-term Targets of the Energiewende, 2016.

[2] Federal Ministry of Economics and Technology (BMWi), Research for an environmentally sound, reliable and affordable energy supply, 2011.

[3] Bundesverband der Energie- und Wasserwirtschaft (BDEW), Technical Guideline Generating Plants Connected to the Medium-Voltage Network, 2008.

[4] Western Electricity Coordinating Council (WECC), WECC Guideline: Central Station Photovoltaic Power Plant Model Validation Guideline. WECC Renewable Energy Modelling Task Force, 2015.

[5] ENERGINET, Smart Grid Technology Demonstration in Denmark for Electric Power Systems with High penetration of Distributed Energy Resources, 2011.

[6] D. Sweeting, Applying IEC 60909, Fault Current Calculations. In IEEE Transactions on Industry Applications, 2012.

[7] VDE – Verband Deutscher, Short circuit currents in three phase a.c. systems - part 0. Calculation of currents (IEC 60909-0:2001), 2001.

[8] I. Kasikci, Short Circuits in Power Systems: A Practical Guide to IEC 60909-0, 2nd Edition. Weinheim, Germany: Wiley-VCH, 2018.

[9] John J. Grainger, Power System Analysis. New York: McGraw-Hill Inc., 1994.

[10] Noblat B. de Metz, Calculation of short-circuit currents. Cahier Technique no. 158, 2005.

[11] VDN, TransmissionCode 2007: Network and System Rules of the German Transmission System Operators, 2007.

[12] Western Electricity Coordinating Council (WECC), WECC PV Power Plant Dynamic Modelling Guide. WECC Renewable Energy Modelling Task Force, 2014.

[13] CIGRE Task Force C6.04, Benchmark Systems for Network Integration of Renewable and Distributed Energy Resources, 2014.

Low-Pressure Plasma Treatment for Germination and Seedling Growth of Seeds High-Voltage, Plasmas Application to Agriculture

Wasit Arworn[1] Ittipat Punlerd[2] Kanyaratt Supaibulwatana[2] Somsak Dangtip[3]

[1]School of Materials Science and Innovation, Faculty of Science, Mahidol University, Nakhon Pathom, Thailand
wasit_arworn@hotmail.com
[2]Department of Biotechnology, Faculty of Science, Mahidol University, Bangkok, Thailand
[3]Department of Physics, Faculty of Science, Mahidol University, Bangkok, Thailand
Center of Nanoscience and Nanotechnology, Mahidol University, Bangkok, Thailand
somsak.dan@mahidol.ac.th

***Abstract*— Low-pressure plasma was developed. A few physical parameters of plasma reactor as the numbers of turns of induction coil was studied. The inductively coupled reactor was connected to a 13.56 MHz radio frequency (RF) generator with 4-turns induction coil. Optical emission spectra (OES) were recorded. The higher intensity is characterized by a higher power of RF generator. They were used for surface modification of various types of seeds (*Andrographis panucilata, Anethum graveolens and Hibiscus sabdariffa*) to increase the germination rate and seedling growth and reduce the germination time. The effect of different RF power at constant working pressure (1.0 mbar) and treatment time (15 sec) were investigated. the low-pressure plasma treatment was a more effective way to increase the germination rate and seedling growth at higher RF power.**

Keywords—Plasma treatment; Seed treatment

X. INTRODUCTION

Low-pressure plasma has been used for a wide range of technological applications for materials processing. RF discharge allows us to produce a large volume of stable plasma [1]. Plasma process used for etching, deposition, ion implantation, surface modification and polymerization to change physical and chemical properties of surface that are interested in research [2-7].

Plasma-surface interactions are critical during plasma processing. Surface reaction mechanism is necessary for understanding the evolution of feature during the various plasma processing step. It can be divided into three main groups: Surface reactions that produce new functional groups and cross linking, polymerization occurs at the surface forming a thin film on the material surface, and Plasma treatment removed material from the surfaces and increased surface roughness by chemical reactions and physical etching [8].

Low-pressure plasma treatment is a fast method to improve seed performance and crop yield. It has essential roles in physiological processes, including reducing the bacteria, changing seed coat structures, increasing the permeability, and seed germination and seedling growth [2]. In addition, plasma treatment also could improve the physiological metabolism of the plant. This effect has been demonstrated in several plants. The plasma has an advantage in uniform treatment, there is no destruction of seeds and plasma process does not require chemicals. The use of chemical treatment can pollute the environment, but no environmental pollutants remain after the treatment.

In this work, we develop the low-pressure plasma applications for surface modification of seeds. The main aim of this study was to develop a system, optimize operating conditions (working pressure, gas flow rate and treatment time) and physical parameter (RF power) in low-pressure plasma to increase the germination rate, seedling growth and reduce germination time with different RF power at constant working pressure and treatment time. The increase in germination rate and seedling growth and reduction in the germination time of seeds is useful and cost-effective growth of the crop products.

XI. MATERIALS AND METHODS

Plasma Reactor

A schematic of low-pressure RF plasma was shown in Fig. 1. Plasma is generated in borosilicate glass discharge tube with a diameter of 80 mm and length of 20 cm in horizontal direction. A 5 mm diameter of induction copper coil is mounted around the discharge tube. The coupling set up consists of a RF power generator (CESAR, Advance Energy, China) and a matching network (VM600A, Advance Energy, China) at a frequency of 13.56 MHz. The applied RF powers were varied as 40, 60 80 and 100 W with the same working pressure and treatment time. A vacuum system

consists of a rotary pump (E2M5, Edwards, USA) and a cross-section speedivalve that separates the plasma chamber from the filtration unit and control the flow of plasma gas. The flow rate of ambient air and argon (Ar) gas are controlled by mass flow controller to maintain the total working pressure of system. The seed samples were placed on glass plate (50 mm x 75 mm) at the center of plasma chamber. Plasma species and the characteristic of RF discharge are investigated by optical emission spectroscopy (OES) in the range of 300 nm to 900 nm that were collected by a spectrometer (USB 4000, Ocean optic, USA) via a fiber optic.

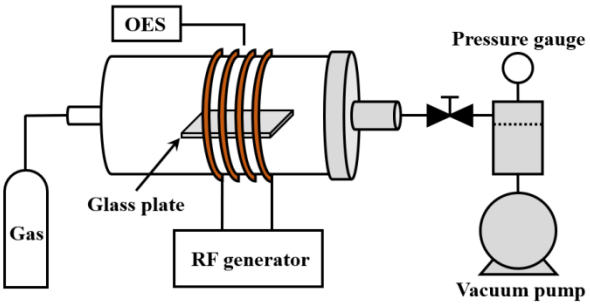

Fig 1. Schematic of experimental set up

Seed Treatment

The investigation was designed to test the effect of plasma treatment on seed survival after 14 days and seedling growth after 20 days after plasma treatment. The plasma treatment would react with the surface of the seed. Seed of chiretta (*A. panucilata*) (*n=30*, size 1.0-1.3 mm), dill (*A. graveolens*) (*n=30*, size 3.0-5.0 mm) and roselle (*H. sabdariffa*) (*n=10*, size 3.0-5.0 mm) were treated for 15 sec with Ar, but for various RF power: 40, 60, 80 and 100 W compared with the control seeds (Vacuum treatment: without plasma ignition, were summitted to the same vacuum and gas flux as the treated seeds). The total working pressure during the discharge was maintained at 1.0 mbar.

XII. RESULTS AND DISCUSSIONS

Characteristic of Plasma

Plasma is discharged with RF generator and matching network assembly. The RF power is transferred to the reactor through induction coil as a coupling electrode. The characteristics of the suitable induction coil depends on a diameter of discharge chamber. The lower number of turns of induction coil required the lower RF power to ignite plasma as shown in Table I. On the other hand, the number of turns of the induction coil is too small, the reflected power is increased. Because of the limitation of matching circuit, low-impedance induction coil cannot receive the RF power, efficiently. The lower starting power means that plasma can be sustained at the lower power and get higher intensity at the same RF power. The 4-turns (copper) induction coil was chosen for seed treatment because it required a low starting power and the reflected power was less than 1%.

TABLE III.
STARTING POWER OF PLASMA INITION IN EAECH COUPLING ELECTRODE

Coupling electrode	Starting power (W)
2-turns coil	12.67±0.58
4-turns coil	14.67±0.58
6-turns coil	16.33±0.58
8-turns coil	23.67±1.17

The atomic emission igniting from discharge is collected and transmitted to the spectrometer via optical fiber with a window beside reaction chamber. The spectrum emission of discharge was characterized by measuring the wavelength and intensities of emission line with 4-turns induction coil. Optical emission spectra of argon and ambient air plasma are shown in Fig. 2 at the same input power of 100 W. Some of emission line of ambient air plasma and strong argon emission line (313.9 nm) are also observed in argon plasma that cause the surface chemical and physical properties of seeds to change. Fig. 3 shows Ar (313.9 nm) peak intensity as a function of RF power. The emission intensity is getting higher, significantly when RF power is increased. This is considered due to higher RF power accelerating electrons and more collisions.

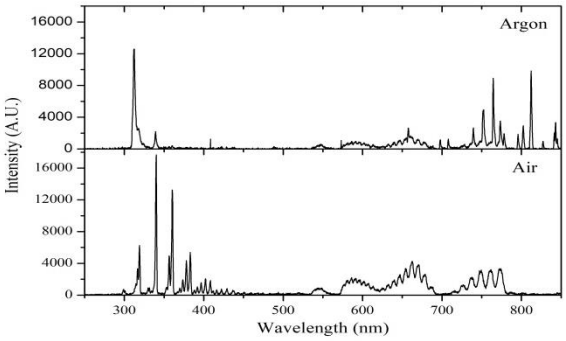

Fig. 2 Emission spectra of argon and air plasma at 100 W

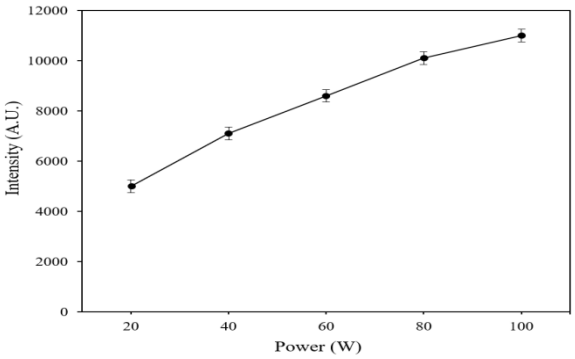

Fig. 3 Evolution of Ar (313.9 nm) peak as a function of power

Seed Treatment

Three types of seed (*A. panucilata*, *A. graveolens* and *H. sabdariffa*) were investigated for germination rate and seedling growth after plasma treatment with 4-turns inductive coil at different RF power ,compared with the untreated-control seeds (vacuum treatment).

1) Germination rate

In this study, germination rate was shown as a percentage of survival seeds after 20 days after plasma treatment. In Fig.4, the germination rate of *A. panucilata* and *A. graveolens* were significantly increased from 23.3% and 20.0% to 56.7% and 46.7%, respectively compared with the control seeds at 100 W. It's indicated that the plasma treatment could promoted the germination of *A. paniculate* and *A. graveolens* seeds. The size of seeds was not related to germination improvement, when RF power increased. On the other hand, the germination rate of *H. sabdariffa seeds* was increased from 60.0% to 100% compared with the control seeds at 40 W. Then, the germination rate was decreased at higher RF power. Therefore, the specific genotypic effect may cause to germination response differentiation. The suitable dose should be required for each type of seeds. Moreover, a plasma treatment with lower or higher energy levels had no significant influence on seed germination

2) Seedling growth

The effect of plasma treatment on seedling growth performance of seeds were analyzed using root and shoot length data as shown in Fig. 5 and 6. The seedling of *A. paniculate* (Fig.7) showed the most increasing of growth effect in root length. The root length was significantly increased from 0.5 cm to 1.9 cm at 80 W and decreased to 0.9 cm at 100 W. The shoot length of *A. paniculate* also increased up to 1.4 cm at 60 W. Then, decreased with RF power higher than 80 W. For *A. graveolens*, the length of root was suddenly increased up to 2.1 cm at 60 W, compared with the control seeds. However, there are no significant effect on shoot growth until the RF power up to 80 W. Overall, the length of root of *A. paniculate* and *A. graveolens* increased more than the length of shoot, compared with the control. In contrast, the effect of plasma treatment on root growth of *H. sabdariffa* seed had no significant different. Moreover, the shoot length was decreased after plasma treatment. Effect of cold plasma was more dramatic on root growth than shoot growth. The specific genotypic effect may cause to germination response differentiation. Plasma treatment with lower or higher energy levels had no significant influence on seed germination

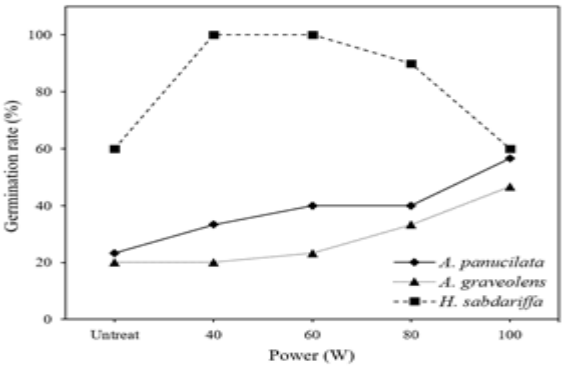

Fig 5. Percent germination of plasma-treated and control seeds of *A. panucilata*, *A. graveolens* and *H. sabdariffa* after 20 days at different RF power

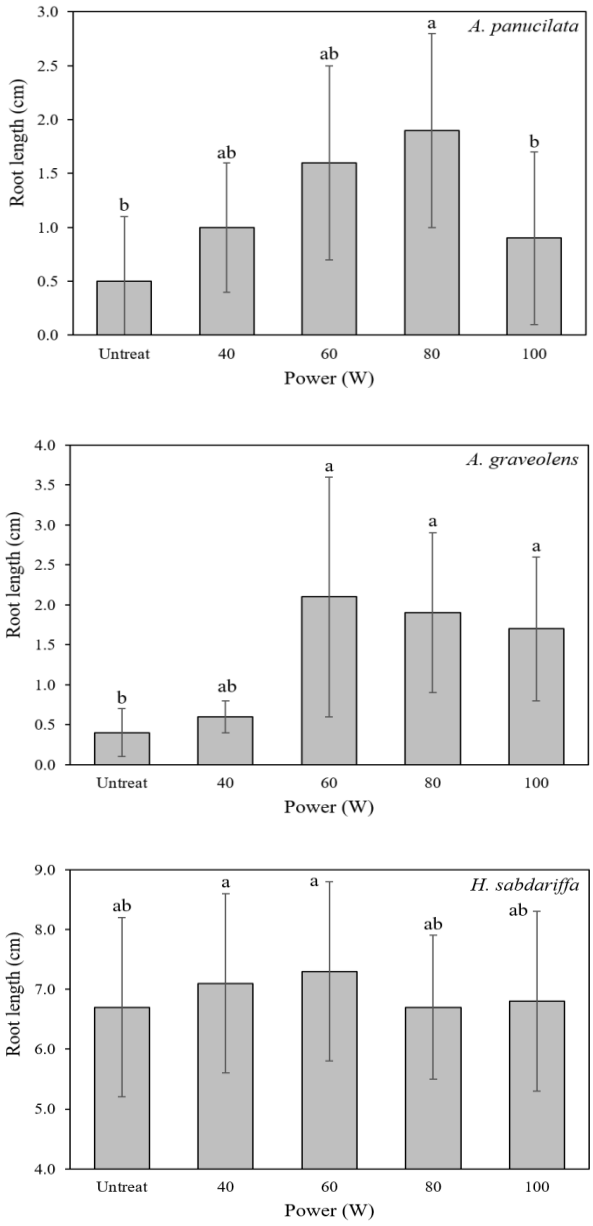

Fig 4. Average root length of plasma-treated and control seeds of *A. panucilata, A. graveolens and H. sabdariffa* after 20 days at different RF power

*Means with the different superscripts are significantly different

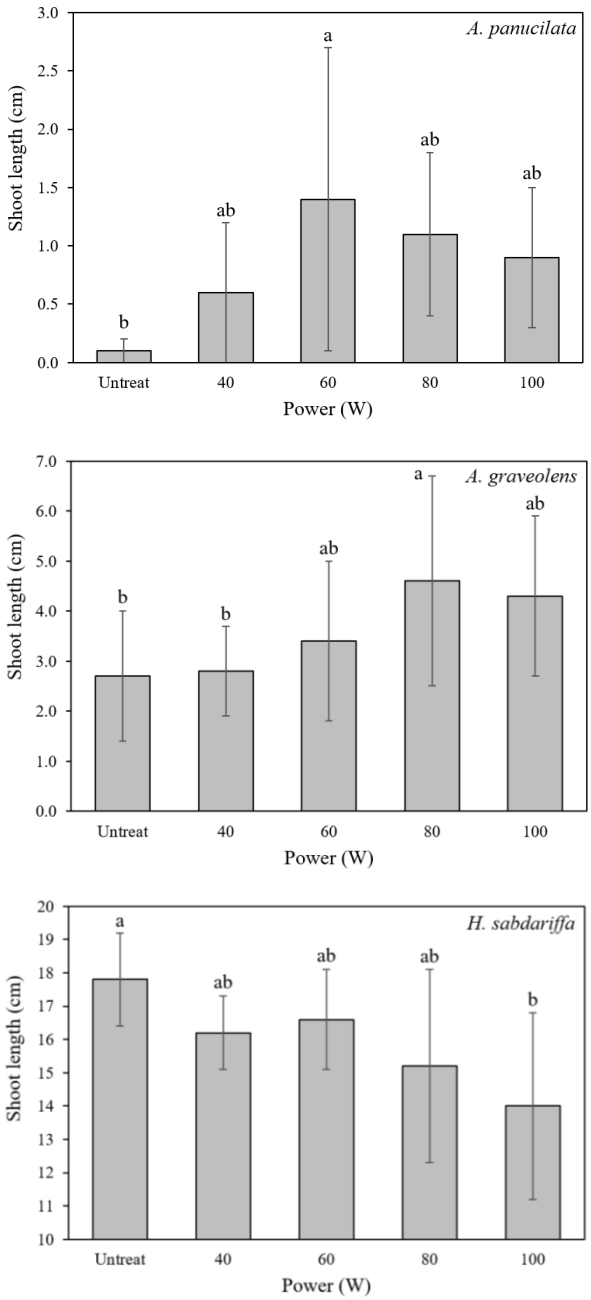

Fig 6. Average root shoot of plasma-treated and control seeds of *A. panucilata, A. graveolens and H. sabdariffa* after 20 days at different RF power

*Means with the different superscripts are significantly different

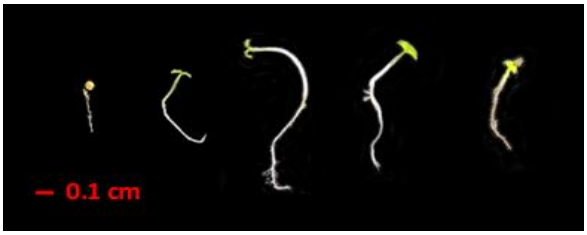

Fig 7. Seedling growth of *A. panucilata* after 20 days after plasma treatment with (left to right) control, 40, 60 80 and 100 W

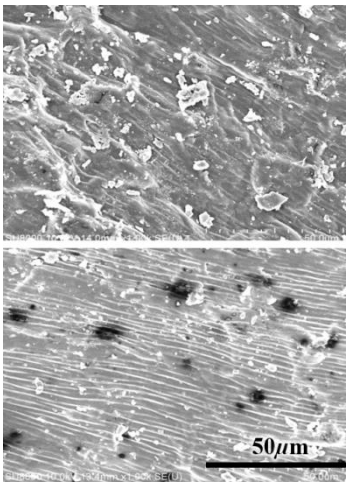

Fig 8. SEM image of *A. graveolens* seed before (upper) and after (lower) plasma treatment at 80 W

The scanning electron microscope images revealed many pores on the seed coat surface on dorsal side of *A. graveolens* as a candidate seed with recommended RF power at 80 W after plasma treatment compare with control seed. After plasma treatment, Grain surface was burn and look smoother than control seed. Plasma treatment removed material from the surfaces by physical etching.

XIII. CONCLUSIONS

We have studied characteristics of plasma, seed germination and seedling growth by applied the different RF power via low-pressure plasma. In this series of studies, we operated the low-pressure plasma with 4-turn induction coil that suitable for reactor geometry. The germination rate was indicated that the plasma treatment could promoted with higher RF power. The size of seeds was not related to germination improvement. However, if the plasma treatment used a lower or higher energy level then no significant effect was observed on seedling growth. Effect of cold plasma was more dramatic on root growth than shoot growth. These criteria are considered a necessity for future development.

Acknowledgment

The author would like to thank the Development and Promotion of Science and Technology Talents Project (DPST) and Center of Nanoscience and Nanotechnology (Mahidol University) for financial support.

REFERENCES

[1] Konuma, M. (2005). Plasma techniques for film deposition. Alpha Science International.

[2] Ling, L., Jiafeng, J., Jiangang, L., Minchong, S., Xin, H., Hanliang, S., & Yuanhua, D. (2014). Effects of cold plasma treatment on seed germination and seedling growth of soybean. Scientific reports, 4, 58-59.

[3] Bormashenko, E., Grynyov, R., Bormashenko, Y., & Drori, E.(2012). Cold radiofrequency plasma treatment modifies wettability and germination speed of plant seeds. Scientific reports, 2, 741.

[4] Dhayal, M., Lee, S. Y., & Park, S. U. (2006). Using low-pressure plasma for Carthamus tinctorium L. seed surface modification. Vacuum, 80(5), 499-506.

[5] Volin, J. C., Denes, F. S., Young, R. A., & Park, S. M. (2000). Modification of seed germination performance through cold plasma chemistry technology. Crop Science, 40(6), 1706-1718.

[6] Sera, B., Spatenka, P., Sery, M., Vrchotová, N., & Hruskova, I. (2010). Influence of plasma treatment on wheat and oat germination and early growth. IEEE Transactions on Plasma Science, 38(10), 2963-2968.

[7] Meiqiang, Y., Mingjing, H., Buzhou, M., & Tengcai, M. (2005). Stimulating effects of seed treatment by magnetized plasma on tomato growth and yield. Plasma Science and Technology, 7(6), 3143.

[8] Chan, C. M., Ko, T. M., & Hiraoka, H. (1996). Polymer surface modification by plasmas and photons. Surface science reports, 24(1), 1-54.

Removal of chlorpyrifos in Chinese kale *(Brassica oleracea* var. *alboglabra)* by fine bubble technology

Janyawat T. Vuthijumnonk*
College of Integrated Science and Technology
Rajamangala University of Technology Lanna
Chiang Mai, Thailand
E-Mail: vjanyawat@hotmail.com

Vishnu Tonglek
Faculty of Engineering
Rajamangala University of Technology Lanna
Chiang Mai, Thailand

***Abstract*— Chinese kale production requires various pesticide application. Chlorpyrifos, an organophosphate pesticide, is a commonly used pesticide. This study aimed at investigation of chlorpyrifos-removal effect of fine bubble technology. Three gases were used for microbubble production including air, oxygen and ozone. Chlorpyrifos- contaminated Chinese kales were washed with water contained microbubble (air, oxygen or ozone) then tested for chlorpyrifos residue contamination using GPO-TM kits. The residues were not detected after all microbubble treatments. Air microbubbles was chosen for further analysis using GC. While reverse-osmosis water was not effective in removing the residue, approximately 50% of chlorpyrifos was removed after air microbubble treatment.**

Keywords—Chinese Kale, Chlopyrifos, Pesticide removal, Microbubble Technology

I. INTRODUCTION

Chinese kale (*Brassica oleracea* var. *alboglabra*) also known as gai lan in Chinese, is one of the most consumed vegetable in Thailand. Chinese kale production in Thailand covered area around 30,016 acres with a total production of 102405 tons per annual. The plant can be grown in every part of the country where the central part is a major cultivation area [1].

The plant grows well in strong, moist and organic matter riched soil [2]. However, it is a target of several insect pests including but not limit to leaf eating beetle (*Phyllotreta chontanica* Duvivier & *P. sinuata* Steph.) diamondback moth [*Plutella xylostella* (Linnaeus)], common cutworm [*Spodoptera litura* (Fabricius)] and cabbage looper (*Trichoplusia ni* Hübner). Therefore, chlorpyrifos plays an important role in a Chinese kale production. Twelve pesticide residues were found in Chinese kale samples in Thailand with chlorpyrifos higher than maximum residue limits (MRLs) [3].

Chlorpyrifos is an organophosphate pesticide. Its chemical structure is shown in Fig. 1. Its mode of action is an inhibition of acetylcholinesterase enzyme, causing acetylcholine accumulation. The neurotransmitter accumulation then leads to continuous muscle stimulation and contraction [4].

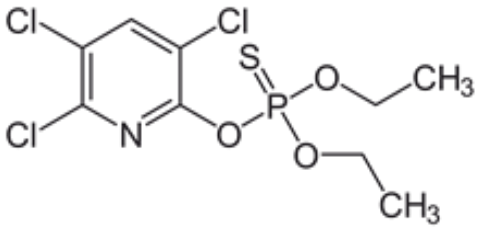

Fig 1. Chlorpyrifos chemical structure

Chlorpyrifos is considered moderate hazardous for living organisms. Symptoms may vary depend on level of exposure. Eye watering, increased saliva and sweating, nausea and headache may be found with mild exposure while intermediate exposure could experience muscle spasms, vomiting and impaired vision. In case of severe poisoning seizures, unconsciousness, paralysis, and suffocation from lung failure are common [5]. Pesticide residues can lead to unfavorable effect on environment and human health. Therefore, a safe method for effective removing of pesticide residue is of interest.

Fine bubble technology is an emerging technique that can be apply in various fields such as agriculture, medicine and engineering. Diameter of the fine bubble ranges from one micrometer to one hundred millimeters. The bubbles can be generated using different types of gas which leads to distinct characteristic of the bubbles. Interestingly, generation of free radicals, self-pressurization and negative surface charge are common characters in microbubbles regardless of gas types [6]. Free radicals generated from microbubble collapsing can deconstruct several chemical compounds including some pesticides. Sole ozone microbubble exhibit fenitrothion-removal property [7]. Moreover, ozone microbubble combined with ultrasonic irradiation technique abolished ethion, an organophosphate pesticide, in tangerine sample without altering any appearances [8].

Government Pharmaceutical Organization of Thailand produced a test kit for detection of four insecticide groups, GPO TM-Kit (Petty patent no. 7554), which is simple to use, budget friendly and readily available. Thin Layer Chromatography (TLC) technique couple with UV (254 nm) reaction were adopted. The result from the kit is rapid but unable to produce quantitative information. In this study, the

kit was therefore, used for screening. The further study with gas chromatography (GC) was carried out to obtain detail information.

Even though, a pesticide-removal effect of fine bubble technology has been documented, to our knowledge, there is no report on removal of chlorpyrifos using the technique. Therefore, this study aims to investigate chlorpyrifos removing effect of microbubble technology along with quantitative analysis.

II. METHODOLOGY

Materials

Chinese kales were purchase from a local market in Chiang Mai, Thailand. The products were kept at 4°C and used in the experiment within 24 hours after purchased. A common organophosphate insecticide, chlorpyrifos (40% w/v), were purchase from Global-crops, Thailand. GPO TM-kits was purchased from the Northern Government Pharmaceutical Organization, Thailand

Preparation of chlopyrifos contaminted Chinese kale

The pesticide was prepared according to the commercial label. The vegetable was immersed in the pesticide solution for 15 min then dried for 30 min at room temperature. After the process, the fruits were separated to five groups which will be subjected to further microbubble treatments. The experimental groups included a control group (C: no further treatment), a positive control group (ROW: treated with Reverse Osmosis-water), an AMB group (treated with air microbubble) and an OMB group (treated with oxygen microbubble).

Treatment with microbubble

Five liters of Reverse Osmosis-water (RO-water) was added in a cylindrical vessel. AMB was generated in the water using an in-house decompression-type microbubble generator (Model: RMUTL-KVM-01) with water flow rate 1.7 L/min, pressure 0.25 - 0.4 mPa, gas flow rate 0.1 L/min. OMB was produced in the same manner with addition of oxygen. Chinese kales (200 g) were immersed to the vessel containing bubbling microbubble for 15, 30 or 60 min.

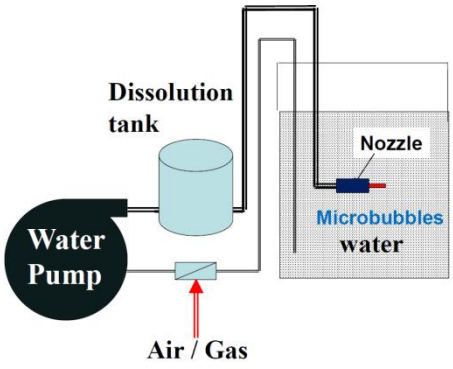

Fig 2. RMUTL-KVM-01 microbubble generator diagram.

Pesticide residue analysis using GPO TM-kit

The treated fruits were tested for pesticide residue contamination as described in the kit manual.

For organophosphate and carbamate detection, the peel sample (5 g) was finely cut and place in 25 mL container. Extracting solution (5 mL) was added to the container followed by 0.25 g activated charcoal powder and mixed thoroughly. The container was left at room temperature for 5 min then the clear part was taken out and dried at 48C. The extracting solution (20 uL) was added to the dried sample and used for TLC analysis. The TLC sheet was until the solvent reached a solvent front line (8.5 cm). The sheet was taken out from the mobile phase then dried at room temperature and sprayed with a testing solution 1. The sheet was then incubated at 37°C for 10 min. Finally, the sheet was sprayed again with a color testing solution then left at room temperature for three min before reading the result. A present of a white spot means the sample is contaminated with organophosphate or carbamate insecticides.

Pesticide residue analysis using GC

Chinese kale sample was cut and blended using a food processor. The homogenized sample was mixed with magnesium sulfate saturated acetronitrile and sodium chloride. The supernatant was transferred to a 50 mL centrifuge tube then mixed with primary–secondary amines (PSA) (50 mg), graphited carbon black (7.5 mg) and magnesium sulfate (150 mg). The mixture was mixed thoroughly and centrifuge. The supernatant was added to a vial for direct injection into the Bruker GC-MS/MS system. Chlorpyrifos detection was performed using a Bruker 456 gas chromatography (GC) coupled with Bruker Scion Triple Quadrupole mass spectrometer (GC–MS/MS). The conditions for chlorpyrifos detection were referred to as in the previous report [9].

Statistical analysis

Data are presented as mean ± standard deviation (SD). Differences between groups were assessed by a one-way analysis of variance (ANOVA), followed by multiple comparisons utilizing Tukey's test. Statistically significant was considered when probability values were less than 0.05. Minitab software version 18 was used for statistical analysis.

III. RESULTS AND DISCUSSION

Chinese kales were treated with chlorpyrifos then washed by water contained microbubbles (air, oxygen or ozone) at 15,30 and 60 mins. At 15 and 30 mins, all microbubble treatments were not effective in removing chlorpyrifos residues however the residues were removed when the treatment time was extended to 60 mins (Table I).

TABLE I
DETECTION OF CHLORPYRIFOS RESIDUE USING GPO-TM KITS

Type of treatment	Time (mins)		
	15	30	60
Control	+	+	+
ROW	+	+	+
AMB	+	+	-
OMB	+	+	-
OzMB	+	+	-

Chinese kale is a commonly used vegetable in Thai cuisine, but its production required pesticide application. Chinese kale samples from local markets in Thailand were found contaminated with chlorpyrifos ranged from 7 – 37,700 ppb [3]. Maximum Residue Limits of chlorpyrifos in Chinese kale is 50 ppb (0.05 mg/kg). The finding in this study agreed with a previous study that the washing period was positively correlated with amount of removed insecticide [10].

Several studies have been proposing various methods for effective removal of chlorpyrifos from agricultural products. Tap water was unable to remove chlorpyrifos in cauliflower samples while tamarind juice with pH 1.88 exhibited chlorpyrifos reducing effect [11]. 2% Acetic acid removed more than 80% chlorpyrifos residue in date samples [12]. Hydrostatic pressure process was also study for its chlorpyrifos-removal effect. The study showed that appearances of the fruits were not affected by the treatment and about 75% of the contaminated pesticide was removed [13]. However, all available proposed cleaning methods are in some extent difficult to carried out. Therefore, a chance of microbubble generator to become a household cleaning method is promising.

According to the screening results, air microbubble was selected for further investigation because it was less complication during preparation and did not required additional equipment eg. oxygen cylinder or ozone generator. Chlorpyrifos-removal effect of air microbubble was confirmed by GC (Fig. 2).

The concentration of a control chlorpyrifos-contaminated sample was 64.84 mg/kg. Washing test revealed that RO-water reduced approximately 20% of chlorpyrifos contamination while air microbubble treatment significantly reduced chlorpyrifos contamination by 50%. A study showed that chlorpyrifos contaminated strawberries could be reduced by 68.1% after washing with tap water. However, a study of chlorpyrifos removal in cauliflower showed that tap water was not effective as a cleaning solution. The controversy may line on the differences between surface type of each plant sample.

In our study, RO-water can reduce chlorpyrifos contamination by 20%. The partially removal-effect may attribute to the nature of chlorpyrifos. The pesticide is a non-systemic where an effect would be found when it comes into direct contact with plant tissues. For this reason, the pesticide residue could partially be removed by simple operations.

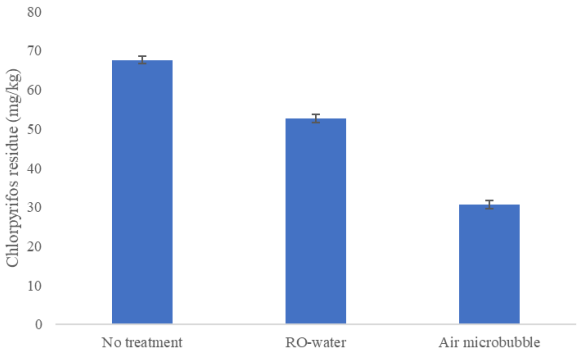

Fig 3. Chlorpyrifos residue (mg/kg) in Chinese kale with different treatments.

In the current study, chlorpyrifos residue was removed by microbubble treatment. Microbubble technology is gaining more attention for its applications in agricultural field because of its unique properties. Microbubble generation is a production of fine bubble size between 1 µm to 100 µm in liquid medium. Generation of free radicals from microbubble collapsing can be observed using an electron-spin-resonance test with a spin-trap reagent (a 5,5-dimethyl-1-pyroroline-N-oxide). Free radicals generated from microbubble decayed several chemical compounds [14]. Organophosphate-removal effect of microbubbles has been extensively studied. Fenitrothion-contaminated lettuce was reduced by 32% after a treatment with bubbling ozone microbubble produced from decompression generator [15]. Similar finding was also found with contaminated persimmon leaves. Ozone microbubble effectively removed more than 40% of fenitrothion where appearance and other quality of the leaves were unchanged [7]. Ethion is an organophosphate-insecticide widely used for tangerine cultivation. Ozone microbubble combined with ultrasonic technique removed more than 70% ethion residue [8]. Previous studies showed that the pesticide-removal property of microbubbles varied. Removal percentage in leaf samples was less than 50% while higher removal percentage was found in waxy sample (tangerine). It is possible that types of plant surface affect pesticide attachment on different surfaces [16].

A clear mechanism of insecticide-removal effect of microbubbles is still unclear, however a possible mechanism has been proposed. Chlorpyrifos degradation in aqueous solution was studied and it revealed that oxidation process contributed to the pesticide degradation [17]. Hydroxyl radicals ($^{\bullet}OH$), generated from excited atomic oxygen in water, have been studied for their destroying effect on organophosphate pesticide molecules including, malathion and chlorpyrifos [18]

Many researches have proposed various way for removing chlorpyrifos residue, mostly required high technology or scientific equipment such as gamma radiation [19], metal-nanoparticles [20]. In this study, an in-house

microbubble generator produced in our laboratory is another alternative. Moreover, previous study showed that acidic condition assisted with chlorpyrifos de-contamination. Therefore, suitable pH and temperature for microbubble generation required further study. This is the first study revealing chlorpyrifos removal effect of microbubbles. In this study, the level of chlorpyrifos residue after washing with microbubbles was yet to meet a requirement for MRLs which might attribute to concentration of the pesticide used during pesticide treatment. Even so, air microbubble reduced approximately 50% of contaminated-chlorpyrifos in Chinese kale samples.

IV. CONCLUSION

Chlorpyrifos, a widely used pesticide, was reduced using microbubble technology regardless of gas type. Time of the treatment positively related with level of chlorpyrifos removed from test samples. Effect of air microbubble on chlorpyrifos removal was observed. The fine bubble technology reduced around 50% pesticide residue from Chinese kale sample after 60 minutes treatment. The most suitable condition for pesticide removal effect of the fine bubble technology and degradation mechanism require further investigation.

Acknowledgment

This project has been granted by National Research Council of Thailand and supported by Rajamangala University of Technology, Lanna.

REFERENCES

[1] "Chinese Kale" Department of Agricultural Extension, Thailand, May 2016, http://www.agriinfo.doae.go.th/year60/plant/rortor/veget/17.pdf, Retrieved 2019-02-01.

[2] R.B. Oyugi, "Peticide residues in some vegetables rotated with tobacco using HPLC, and farmers' awareness of pesticide health effects in Kuria-Migori, KENTA. Pages 1-2. *In: Thesis(BSC., PGDC).* Kenyatta University,Nairobi, Kenya. 2012.

[3] S. Wanwimolruk, O. Kanchanamayoon, K. Phopin, and V. Prachayasittikul, "Food safety in Thailand 2: Pesticide residues found in Chinese kale (*Brassica oleracea*), a commonly consumed vegetable in Asian countries," *Science of the Total Environment*, vol. 1, no. 532, pp. 447-455, June 2015.

[4] "Chlorpyrifos," Pesticide Action Network, http://www.panna.org/resources/chlorpyrifos-facts#2 Retrieved 2019-02-20.

[5] K. Christensen, B. Harper, B. Luukinen, K. Buhl, D. Stone, "Chlorpyrifos Technical Fact Sheet," National Pesticide Information Center, Oregon State University Extension Services. http://npic.orst.edu/factsheets/archive/chlorptech.html. Retrieved 2019-03-16.

[6] A. Agarwal, W. Jern Ng, and Y. Liu, "Principle and applications of microbubble and nanobubble technology for water treatment," Chemosphere, vol. 84, no. 9, pp. 1175-1180, Aug 2011.

[7] H. Ikeura, F. Kobayashi, M. Tamaki, "Removal of residual pesticides in vegetables using ozone microbubbles," J. Haz. Mat., vol. 186, no. 1, pp. 956-959, Feb 2011.

[8] K. Whangchai, J. Uthaibutra, N. Nuanaon, and H. Aoyagi, "Effect of ozone microbubbles and ultrasonic irradiation on pesticide detoxification in tangerine cv. Sai Nam Pung," Inter. Food Res. J., vol. 24, no. 3, pp. 1135-1139, 2017.

[9] M. Duff, and M. Voglino, "Rapid and robust multi-residue pesticides analysis using the Bruker 320-MSGC triple quadrupole mass spectrometer," 2012. http://www.spectroscopyonline .com/ multi-residue-pesticide-analysis-using-gc-triple-quadrupole-mass-spectrometer Retrieved 2019-03-08.

[10] B. Lozowicka, M. Jankowska, I. Hrynko, et al., "Removal of 16 pesticide residues from strawberries by washing with tap and ozone water, ultrasonic cleaning and boiling," Environ. Monit. Assess., vol. 188, no. 51, pp. 1 - 19, Dec 2015.

[11] M.F.M. Nowowi, M.A.M. Ishak, K. Ismail1 and S.R. Zakaria, "Study on the effectiveness of five cleaning solutions in removing chlorpyrifos residues in cauliflower (*Brassica oleracea*)," J. Envi. Chem. Ecotox., vol 8, no. 7, pp. 69-72, July 2016.

[12] K.A. Osman, A.I. Al-Humaid, K.N. Al-Redhaiman, R.A. El-Mergawi., "Safety methods for chlorpyrifos removal from date fruits and its relation with sugars, phenolics and antioxidant capacity of fruits," J. Food Sci. Technol., vol 51, no. 9, pp. 1762–1772, Apr 2012.

[13] T. Iizuka, S. Maeda, and A. Shimizu, "Removal of pesticide residue in cherry tomato by hydrostatic pressure" J. Food Eng., vol. 116, no 4, pp. 796-800, June 2013.

[14] M. Takahashi, K. Chiba, and P. Li, "Free-radical generation from collapsing microbubbles in the absence of a dynamic stimulus," J. Physic. Chem. B, vol. 111, no. 6, pp. 1343–1347, January 2007.

[15] H. Ikeura, S. Hamasaki, M. Tamaki, "Ozone microbubble treatment at various water temperatures for the removal of residual pesticides with negligible effects on the physical properties of lettuce and cherry tomatoes," J. Food Sci., vol. 78, pp. T350-355, February 2013.

[16] A.S. Crafts, and C.L. Foy, (1962) "The chemical and physical nature of plant surfaces in relation to the use of pesticides and to their residues. In: Gunther F.A. (eds) Residue Reviews / Rückstands-Berichte. Residue Reviews / Rückstands-Berichte, vol 1. Springer, New York, NY, vol. 82, no. 8, pp. 1109-1115, Feb 2011.

[17] Y. Zhang, Y. Hou, F. Chen, Z. Xiao, J. Zhang, and X. Hu, "The degradation of chlorpyrifos and diazinon in

aqueous solution by ultrasonic irradiation: Effect of parameters and degradation pathway," Chemosphere, vol. 82, no. 8, pp. 1109 – 1115, Feb 2011.

[18] Y. Zhang, Z. Xiao, F. Chen, Y. Ge, J. Wu, and X. Hu, "Degradation behavior and products of malathion and chlorpyrifos spiked in apple juice by ultrasonic treatment," Ultra. Sonochem., vol. 17, no. 1, pp. 72-77, January 2010.

[19] M.S. Hossain, A.N.M. Fakhruddin, M. Alamgir Zaman Chowdhury, and M. Khorshed Alam, "Degradation of chlorpyrifos, an organophosphorus insecticide in aqueous solution with gamma irradiation and natural sunlight Journal of Environmental Chemical Engineering," J. of Envi. Chem. Eng., vol. 1, no. 3, pp. 270-274, Sep 2013.

[20] M.S. Bootharaju, and T. Pradeep, "Understanding the degradation pathway of the pesticide, chlorpyrifos by noble metal nanoparticles, *Langmuir*, vol. 28, no. 5, pp. 2671–2679, Jan 2012.

Students' Perceptions of Classroom Learning Environment and Approaches to Learning in Printing and Packaging Technology

Inthira Paleenud
Learning Innovation and Technology Program
Faculty of Industrial Education and Technology
King Mongkut's University of Technology Thonburi
Bangkok, Thailand
inthira.pal@mail.kmutt.ac.th

Krittika Tanprasert
Faculty of Industrial Education and Technology,
Learning Institute
King Mongkut's University of Technology Thonburi
Bangkok, Thailand
krittika.tan@mail.kmutt.ac.th

ABSTRACT_The changing world requires workforce with higher order thinking skills and it is believed that this is associated with deep learning approach, which is influenced by classroom learning environment. The goal of this papers was to develop the questionnaire to collect data to investigate the relationship between learning approach and the perceived classroom learning environment. The questionnaire based on modified WIHIC and R-SPQ-2F had good reliability but with slight modification. The sample data collected from 50 junior students from the Department of Printing and Packaging Technology, KMUTT indicated the relationship between deep learning and investigation, teacher support, involvement, task orientation and equity, and cooperation but not student cohesiveness.

Keywords: **Constructivist theory; Perceptions of classroom learning environment; Approaches to learning**

(I) INTRODUCTION

With the world changing at a rapid pace, many jobs today will fade out while many more have yet to emerge. In the near future, a completely different workforce will be needed to serve the society. The expertise as well as the ability to obtain knowledge has become more crucial. It is no longer important to teach students fact as this is available from various sources. It is more critical to promote learning that employs higher order thinking skills. Therefore, the goal of education is shift to promote learning with higher order thinking rather than memorizing [1].

A large number of research has been conducted on students' learning. Approach to learning has been identified as a good description of students' learning and it is helpful in conceiving ways of improving teaching [2]. It also influences learning process which lead to difference in learning outcomes [3]. Approaches to learning are classified into two approaches, deep and surface. Surface approach is an approach in which students' intention is to reproduce the material being studied through memorizing or routinized procedures [4]. Deep approach is characterized by students having an intention to seek meaning and understanding of the material being studied through elaborating and transforming the material [5].

Deep approach promotes high cognitive level than surface approach does, as deep approach supports student's ability to explain, hypothesize, argue and reflect theories. It has been suggested that students who has deep approach to learn can achieve high levels of understanding through applying the hard theories rather than memorizing them. While in surface approach, cognitive levels tend to be lower as students can only memorize and describe the theory, but lack the ability to expand it further [1]. Numerous attempts have been made to optimize students' approaches to learning towards deep, that is associated with constructivist teaching [6]. This teaching strategy put emphasis on learners actively construct knowledge for themselves.

Several studies have been found that students' perceptions of their learning environments, which include various kinds of physical, social and psychological factors have a significant influence on their approaches to learning and the achievement of learning outcome [7]. Higher achievement on a variety of learning outcomes have been associated with students' perception of classroom as having order and organization, cohesion, and goal direction. In addition there have been few attempts to relate approaches to learning to perceptions of the psychosocial environment of classrooms. Dart et al. [8] investigated the relationship between perception of classroom learning environment and approaches to learning of secondary school students. The study indicated that deep approach was significantly related to classroom learning environments which were perceived to be highly personalized, encouraging active participation in the learning process, and, allowing students to use their investigative skills in learning activities.

There are similar research to the aforementioned studies that have been conducted in various geographical location such as US, UK, Netherlands, Australia and developed Asian countries such as Hong Kong, Taiwan, and Singapore. To the best of the authors knowledge, these topics have not been studied in the context of Thai higher education. Therefore, our goal of this research is to develop the data collection tools in Thai language in order to study the following research questions

- What is the relationship between the students' perceptions of classroom learning environment and students' approaches to learning?
- Which dimensions of learning environment enhances deep approach to learning?

In the scope of this paper the research question focus on junior students in the Department of Printing and Packaging Technology, King Mongkut's University of Technology Thonburi.

(II) HYPOTHESIS

The perceptions of classroom learning environment were significantly related to approaches to learning of the third year students in the Department of Printing and Packaging Technology, King Mongkut's University of Technology Thonburi.

(III) LITERATURE REVIEW

The constructivist learning theory defines learning as an 'active process in which learners are active sense makers who seek to build coherent and organized knowledge [9]. How this theory is put into practice is being debated. Some researchers indicated that active knowledge construction could take place in any teaching method even while attending a lecture [10]. Others argues teaching strategy must be applied or designed in order to support students to construct knowledge for themselves [11]. These constructivist teaching strategies are typically student-centered. Students are also expected to be active participants rather than passive recipients of new information. Some of the teaching strategies that has been employed for constructivist are problem-based learning, project-based learning, case-based learning and inquiry-based learning.

The concept of approaches to learning originated from Marton and Saljo [12]. They used a phenomenographic theory research approach to examine how students learn from text provided. They observed that students responded in two distinct ways. One group remembered a list of disjoined fact and did not comprehend the point author was making. This group uses surface learning approach. The other group concentrate their effort to understand the meaning of the author's message. This corresponds with deep approach to learn [12]. This conceptual framework became know as 'Student Approaches to Learning' (SAL) theory [13], which characterize approach to learning as surface and deep approaches.

Students with surface approach intends to reproduce the material being studied through memorization or routinized procedure. This approach have been linked to the traditional transmission model of teaching, which information is transferred from teachers to learners and learners [6] such as chalk and talk approach.

Students with deep approach is characterized by those who intended to seek meaning and understanding of the material being studied through elaboration and transforming the material. This approach to learning is associated with constructivist teaching which emphasises that learners actively construct knowledge for themselves [5].

(IV) RESEARCH METHOD

(4.1) Sample

The sample group for the study was third year students in Department of Printing and Packaging Technology, Faculty of Industrial Education and Technology, King Mongkut's University of Technology Thonburi. (N = 50, Males = 26%; Females = 74%)

(4.2) Instruments

The instrument used for this experiment was questionnaire, which is divided into three parts: general information, classroom environment, and approach to learning. The first section of the survey asked about participant general information including gender and grade point average (GPAX).

The second section of the survey assessed perceptions of classroom learning environment. The questions in this section was translated in Thai language and slightly modified from WIHIC (What Is Happening In This Class?) questionnaire developed by Fraser et al. [14]. The name and number of sub-scale of learning environment (7) and number of items in each sub-scale (8) were the same as in WIHIC. The seven sub-scale of WIHIC questionnaire were: student cohesiveness, teacher support, investigation, involvement, task orientation, cooperation, and equity. The slight modification is that this section asked students to think of their learning environment for all courses in their major (printing and/or packaging courses) rather than experience in a particular course as originally stated in WIHIC. Participants were asked to rate the frequency of each item according 5-points scale with 1 being never and 5 being almost always.

The third section of the survey assessed approaches to learning. This section is directly translated from The revised Two-factor Study Process Questionnaire (R-SPQ-2F) developed by Biggs et al. [2]. This section had 10 items for deep and another 10 for surface approach. Participants were asked to rate the frequency of each item in the same manner as in the second section.

(V) ANALYSIS

Cronbach's alpha coefficient was used as the measurement of reliability of the scale for items in Section 2 and Section 3 of the questionnaire. Cronbach's alpha was calculated separately for each sub-scale for Section 2 and for deep and surface approach for Section 3. It was performed using SPSS Statistics.

Simple correlation analysis was used to examine the bivariate relationship between the students' perceptions of

classroom learning environment and students' approaches to learning. This was performed by peason correlation.

(VI) RESULTS

(6.1)Scale Reliability

Scale reliability was measured using Cronbach's alpha coefficient for the each sub-scale for classroom learning environment (Table 1) and deep and surface approach (Table 2). The coefficient for each sub-scale for classroom learning environment ranged from 0.79 – 0.90 indicating that the scale of all items were reliable as the value of the coefficients were greater than 0.7 [15].

The Cronbach's alpha coefficient of items in surface approach was greater than 0.7 implying that the scale is reliable. However, the coefficient for 10 items in deep approach was 0.53 indicating that some of the items may not be appropriate. It was identified that the question "I feel that virtually any topic can be highly interesting once I get into it" is the outlier. The Cronbach's alpha coefficient was recalculated without the aforementioned item and the value was greater than 0.7 indicating that the scale is reliable.

Table 1 Cronbach's Alpha of Students' Perceptions of classroom Learning Environment

Construct	*Cronbach's alpha*
Student cohesiveness	0.786
Teacher support	0.868
Investigation	0.895
Involvement	0.842
Task orientation	0.841
Cooperation	0.887
Equity	0.868

Table 2 Cronbach's Alpha of Students'Approaches to Learning

Construct	*Cronbach's alpha*
Deep approach	0.838
Surface approach	0.837

(6.2)Relationhsip between Classroom Learning Environment and Learning Approach

The relationship between classroom learning environment and learning approach was measured with Pearson correlation coefficient (Table 3). It was noticed that most of the relationship between surface approach and classroom learning environment were not statistically different ($p > 0.05$) except for the sub-scale of investigation. The positive correlation shows that if students perceived the nature of investigation in the classroom it would shift them toward a more surface learning. However, this same sub-scale also had statistically significant and positive relationship with deep learning approach but with a bigger magnitude of correlation coefficient.

In addition to "investigation" sub-scale, there are 4 classroom learning environment that have a positive statistically significant correlation at the similar level ($p < 0.01$) with deep approach: teacher support, involvement, task orientation, and equity. Another weaker but still significant correlation ($p < 0.05$) was observed between cooperation and deep approach to learn.

TABLE 3 Correlation between Students' Perceptions of Classroom Learning Environment and Students' Approaches to Learning

Classroom learning environment	**Correlation with component of approaches to learning**	
	Deep approach	***Surface approach***
Student cohesiveness	-0.055	0.047
Teacher support	0.529**	-0.256
Investigation	0.417**	0.289*
Involvement	0.404**	0.087
Task orientation	0.520**	-0.071
Cooperation	0.342*	-0.090
Equity	0.564**	-0.118

*P < 0.05; **P < 0.01

(VII) DISCUSSION

In this research we have developed questionnaire in Thai language based on WIHIC and R-SPQ-2F questionnaire. Our results show that WIHIC and R-SPQ-2F questionnaire had good reliability. Although prior researches translated into other language, the results show good reliability as well. Such as WIHIC translated into Arabic [16] and R-SPQ-2F translated into Dutch [17]. The important factors that make these questionnaires reliable are simple context and matching of teaching environment.

According to several studies have been found that students' perceptions of their learning environments have a significant influence on their approaches to learning. Moreover, Dart et al. [8] found that classroom perceived as having higher levels of personalization, participation and investigation are associated with students reporting a deep approach to learning. Also, this study is consistent with the previous findings. We found that the classroom perceived in dimensions of 1) teacher support; teacher helps and care about students well-being 2) investigation; students explore and experiment on their study 3) involvement; students interaction, discussion and enjoy in the class 4) task orientation; students put a lot of effort on their assign tasks and 5) equity; equal treatment of students in classroom such

as compliment and give opportunities to be discuss are associated with deep approach to learning.

REFERENCES

[1] J. Biggs, and C. Tang, Teaching for Quality Learning at University (3rd ed.), New York, The McGraw-Hill Company, 2007.

[2] J. Biggs, D. Kember, and D. Y. P. Leung, "The revised two-factor study process questionnaire: R-SPQ-2F," British Journal of Educational Psychology, 71, pp. 133-149, 2001.

[3] N. Entwistle, "Promoting deep learning through teaching and assessment: conceptual frameworks and educational contexts," TLRP Conference, Leicester, November, pp. 1-12, 2000.

[4] M. Baeten, F. Dochy, K. Struyven, P. Parmentier and A. Vanderbruggen, "Student-centred learning environments: an investigation into student teachers' instructional preferences and approaches to learning," Learning Environments Research, pp. 43-62, 2016.

[5] J. Biggs, "Approaches to the enhancement of tertiary teaching," Higher Education Research and Development," 8, 1, pp. 7-25, 1989.

[6] B. Dart, "Adult learners' metacognitive behaviour in higher education," Adult learning: a reader, pp. 30-43, 1997.

[7] L. Liu and B.J. Fraser, "Development and validation of an english classroom learning environment inventory and its application in china," Application of Structural Equation Modeling in Educational Research and Practice, pp. 75-89, 2013.

[8] B. Dart, P. Burnett, G.B. LEWIS, J. Campbell, D. Smith and A. McCrindle, "Classroom learning environment and students' approaches to leaning," Learning Environments Research, 2, pp. 137-156, 1999.

[9] M Hannafin, J. Hill and S. Land, "Student-centered learning and interactive multimedia: Status, issues, and implications. Contemporary Education," 68(2), pp. 94–99, 1997.

[10] A. Renkl, "Why constructivists should not talk about constructivist learning environments: A commentary on Loyens and Gijbels, Instructional Science," 37, pp. 495–498, 2008.

[11] M. Baeten, F. Dochy and K. Struyven, "Enhancing students' approaches to learning: the added value of gradually implementing case-based learning," European Journal of Psychology of Education, 28, pp. 315-336, 2013.

[12] F. Marton and & R. Saljo, "On qualitative differences in learning-II outcome as a function of the learner's conception of the task," British Journal of Educational Psychology, 42 (2), pp. 115-127, 1976.

[13] J. Biggs, "From theory to practice: A cognitive systems approach," Higher Education Research and Development, 12, pp. 73-86, 1993.

[14] B.J. Fraser, C.J. McRobbie and D.L. Fisher, " Development, validation and use of personal and class forms of a new classroom environment instrument," Paper presented at the annual meeting of the American Educational Research Association, New York, 1996.

[15] D. George and P. Mallery, "SPSS for Windows step by step: A simple guide and reference," 17.0 update, 10th ed., Boston: Allyn and Bacon, 2010.

[16] E. Afari, J.M. Aldridge, B.J. Fraser and M.S. Khine, "Students' perceptions of the learning environment and attitudes in game-based mathematics classrooms," Learning Environments Research, 2012.

[17] D. Gijbels, G.V. de Watering, F. Dochy and P.V. den Bossche, "The relationship between students' approaches to learning and the assessment of learning outcomes," European Journal of Psychology of Education, pp. 327-341, 2005.

[18] M. Baeten, E. Kyndt, K. Struyven, and F. Dochy, "Using student-centred learning environments to stimulate deep approaches to learning: Factors encouraging or discouraging their effectiveness," Educational Research Review, 5, pp. 243-260, 2010.

[19] K.J. Herrmann, A.B. Elsborg and V.M. Cune, "Investigating the relationships between approaches to learning, learner identities and academic achievement in higher education," Higher Education, 74, pp. 385-400, 2017.

[20] D. Kember, "Interpreting student workload and the factors which shape students' perceptions of their workload," Higher Education, 29 (2), pp. 165-184, 2004.

The influence of O_2-Ultra Fine Bubble on the Growth of Wasabi

Toshiki Murai[1], Setsuko Koura[1]

[1]Chiba Institute of Technology / Graduate School of Engineering
Chiba Institute of Technology / 2-17-1 Tsudanuma Narashino Chiba Japan
line 3-City, Country
E-Mail: s1523226TP@s.chibakoudai.jp

Abstract*— Currently, the production volume of wasabi in Japan is decreasing, and the production of rhizomes is less than half compared with the peak period. Thus we focused on Ultra Fine Bubble water. O_2-Ultra Fine Bubble water has been found to increase the germination rate of plants and to exhibit a growth promotion effect on plants. Therefore, in this study, we examined the influence of O_2-Ultra Fine Bubble water on the growth of wasabi.

Keywords*— Ultra Fine Bubble, wasabi, wasabi greens, The germination rate, reactive oxygen

I. INTRODUCTION

Wasabi is a cruciferous plant native to Japan, and is used as a spice to accompany buckwheat noodles and sushi. Wasabi is one of the few plants believed to be domesticated in Japan, and has played an important role in the Japanese food culture. However, the production in Japan, the country of origin, is decreasing year by year, and the production of rhizomes is less than half compared to the peak period. Therefore, it is thought that it is necessary to raise the production amount of wasabi and to provide a stable supply. Since wasabi causes self-poisoning by secreting a component called allyl isothiocyanate during its growth, and hinders its own growth, it is necessary to keep the water clean when cultivating wasabi. It is said that wasabi usually takes about 2 years to harvest, and it has been found that the more oxygen there is in the water, the better it grows. Thus we focused our attention on Ultra Fine Bubble (UFB). O_2-UFB water has been reported to have physiologically active effects such as increasing the germination rate of plants and the survival rate of fishes.

Wasabi native to Japan is cultivated in water and fields, and is classified into two types, "water wasabi" grown in water and "field wasabi" grown in fields. Most plants have VA bacteria in their roots. VA bacteria are symbiotic bacteria that provide phosphorus and nitrogen from the soil instead of receiving sugars from plants. However, wasabi does not have VA bacteria. Therefore, in order to preferentially secure nutrients in the soil, it releases allyl isothiocyanate from the roots to prevent other plants with other VA bacteria from getting close to each other, but when grown in upland fields, wasabi itself also undergoes self-poisoning. The rhizomes can then not grow. On the other hand, since water wasabi is cultivated in a well-drained rice field where fresh water flows, allyl isothiocyanate around the roots can be washed away and the rhizomes can become large without self-poisoning.

The embryo remains in the mother strain for a long time and continues the seed formation phase even after acquiring germinability through cell division and morphogenesis. Seeds with germinability stop cell division and become dry seeds the through accumulation of storage substances such as proteins, lipids and starch, acquisition of drought tolerance and induction of dormancy. Once the seeds germinate and root out, they have to grow while adapting their life cycle to the local environment. Therefore, the seeds sense various external environments such as water, oxygen, and temperature, and select whether to germinate or stay dormant based on a comprehensive judgment. Seed diapause and germination are known to be promoted by abscisic acid and gibberellin, respectively, in various plant species, and the balance between the amount and sensitivity of these hormones plays an extremely important role in the selection of diapause and germination. The dormant seeds will remain dormant unless the conditions for germination are met. In seeds that are not suitable for germination, a suppressive hormone called abscisic acid is generated in the embryo. This abscisic acid promotes the expression of the LEA gene. The gene eventually becomes a protein, and this LEA protein acts to maintain dormancy (Fig.1).

When the water, oxygen, and temperature necessary for germination are accepted in the embryo, an accelerating hormone called gibberellin is synthesized and secreted into the aleurone layer. Amylase is then secreted from the aleurone layer and the starch contained in the endosperm is a decomposed into sugar. This sugar is absorbed by the embryo and the embryo develops with the sugar. In addition, the decomposition of starch into sugar increases the osmotic pressure in the seeds, thereby breaking the hard seed coats and germinating them (Fig.2).

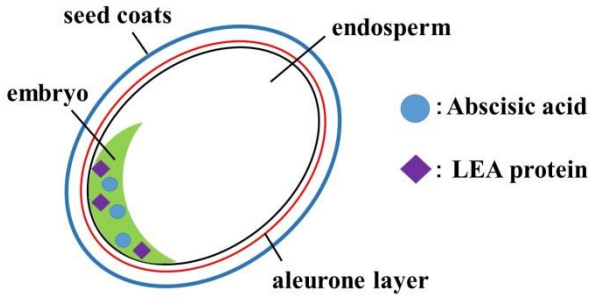

Fig.1 Seed dormancy mechanism

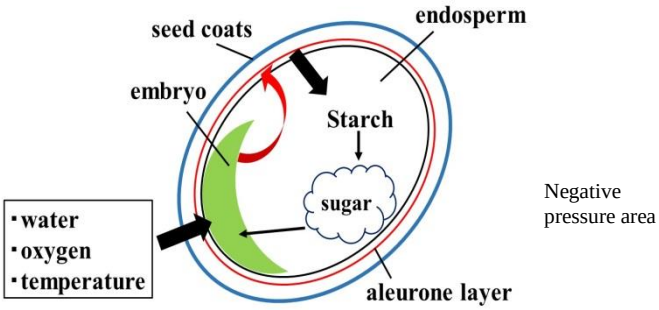

Fig.2 Seed germination mechanism

A bubble having a diameter of 100 to 1.0 μm is called a microbubble, and a bubble having a diameter of 1.0 μm or less is called a UFB. The UFB can be present in high concentrations in water for a long time, and its effects in a wide variety of fields such as agriculture, fishery and medicine (sterilization) have been reported. Normal bubbles rise and disappear, but microbubbles rise slower than normal bubbles, and the UFB does not rise. The UFB can be stored in closed water and in static water, and will remain stable for several months if it does not undergo significant stimulation.

Therefore, in this study, we examined the influence of O_2 -UFB water on the growth of wasabi. We also conducted experiments with wasabi greens, which has a short period until harvesting in parallel with wasabi.

II. PROCESS

II-I Method of producing O_2-UFB

Using the compact UFB generator (Fig. 3), it was fabricated under the conditions listed in Table 1.

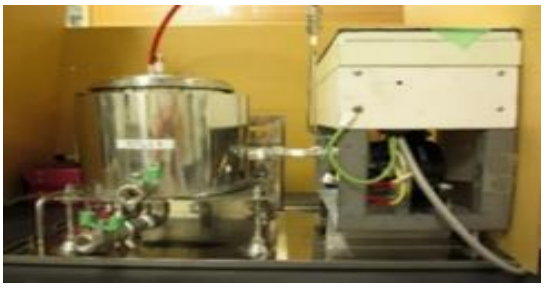

Fig.3 compact UFB generator

Table 1 UEB water Production conditions

Pure water	1L
Gas spices	O_2(purity99.99 %)
Rotation speed	4000 rpm
time	10 min

A schematic diagram of the formation of the UFB by the gas-liquid mixing shear method is shown in **Fig.4**. Gas and liquid come from the IN side. Micro-bubbles generated by mixing them are sent to the UFB generator at pump pressure. The microbubbles are sheared by centrifugal force to generate the UFB.

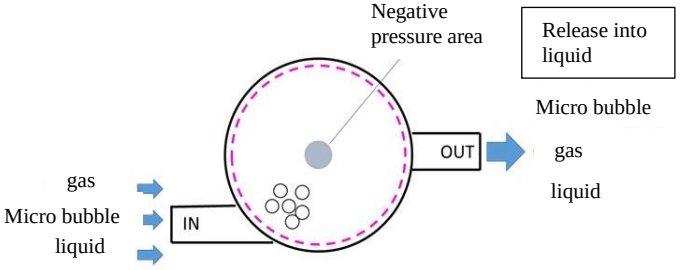

Fig.4 Generation of UFB by gas-liquid mixing shear method

II-II How to grow wasabi greens

The seeds of the wasabi greens were grown under three conditions of 4000mL of O_2-UFB, pure water, and one month after the production O_2-UFB (1M O_2-UFB). The wasabi green was grown using the hydroponic culture kit shown in **Fig.5**. The germination rate in each nutrient solution after 3 days was measured as a comparison of the growth. After measuring the germination rate, 34 g of fertilizer was added, and growth of the wasabi greens was

observed for 25 days under the conditions of 16 hours of light and 8 hours of dark. On the 10th day of the growth, thinning was carried out, and 10 good strains of each nutrient solution were left for the experiment. In addition, we replaced each nutrient solution with a new one every 72 hours. The wasabi greens were grown under the conditions listed in **Table 2**.

Table 2 How to grow wasabi greens

Nutrient solution	O_2 -UFB	pure water	1M O_2-UFB
Fertilizer (g)	34		
Temperature (K)	293.15~298.15		
Water temperature (K)	288.15~298.15		
Amount of water (mL)	4000		
Light period (h)	16		
Dark period (h)	8		

Fig.5 Hydroponic cultivation kit

II-III Measurement of pH and electric conductivity of nutrient solution

The pH and conductivity of the nutrient solution used to grow the wasabi greens were measured. Since the nutrient solution was replaced every 72 hours, the numerical values of the nutrient solution at the time of replacement and the nutrient solution 72 hours after replacement were measured. The pH was measured using a COMPACT pH METER B-71X (manufactured by Horiba, Ltd.). The electrical conductivity was measured using a COMPACT CONDUCTIVITY METER B-771 (manufactured by Horiba, Ltd.).

II-IV How to grow wasabi

The wasabi seeds were planted in separate sprout pots of O_2-UFB and pure water, grown in the dark for 9 days, and the germination rate was measured. Each nutrient solution was replaced with a new one every 72 hours. The wasabi were grown under the conditions listed in **Table 3.**

Table 3 How to grow wasabi

Nutrient solution	O_2 -UFB	pure water
Temperature (K)	285.15~288.15	
Water temperature (K)	288.15~291.15	
Amount of water (mL)	400	

II-V Measurement of water absorption of wasabi seeds

Twenty a wasabi seeds were soaked in each nutrient solution for 90 minutes. From the difference in the total weight before and after soaking the seeds, the water absorption of the seeds in each nutrient solution was measured. The weight of the seeds was measured using a LIBROR AEL-200 (Shimadzu Corporation).

II-VI Confirmation of the existence of reactive oxygen in the wasabi seeds

Twenty wasabi seeds were soaked in 400 mL each of the oxygen UFB water and pure water for 3 days. After that, soaked in the NBT solution made by adding 0.0818 g of Nitro Blue Tetrazolium (NBT) to 100 mL of Tris-HCl buffer for 4 hours. The seeds were then cut with a cutter, and the inside of the seeds observed using an optical microscope.

III. RESULTS AND DISCUSSION

III-I Influence of O_2-UFB on the growth of the wasabi greens

The germination rate of the wasabi greens from each nutrient solution is shown in **Fig.6**. The germination rate of the wasabi greens in each nutrient solution was 89% for 1M-O_2-UFB, 88% for O_2-UFB and 78% for the pure water. From this result, O_2-UFB was thought to show a growth promoting effect on the wasabi greens. Moreover, although the dissolved oxygen content of the O_2-UFB was about 40 ppm, the dissolved oxygen content of the 1M-O_2-UFB was about 8 ppm, thus the O_2-UFB has a growth promoting effect on the plants regardless of the oxygen content.

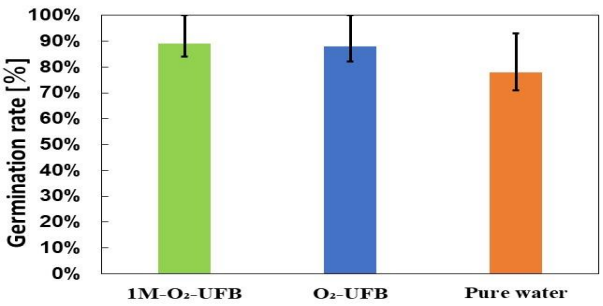

Fig.6 The germination rate of wasabi greens of each nutrient solution

Changes in the size of wasabi greens after germination are shown in **Fig.7**. From **Fig. 7**, it was found that the growing speed of the wasabi greens increases by growing in the O_2-UFB water. Based on these results, it was found that the O_2-UFB water has a growth promoting effect on the wasabi greens.

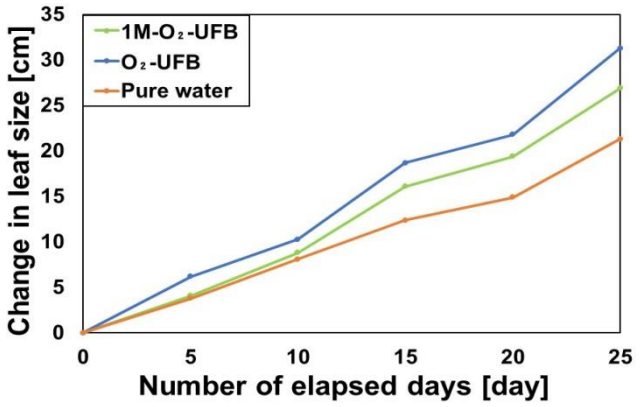

Fig.7 Change in leaf size of each nutrient solution

III-II Measurement of pH and electric conductivity of each nutrient solution

The amount of change in the pH of each nutrient solution is shown in **Fig.8**. The pH of each nutrient solution at the time of replacement was weakly acidic due to the fertilizer, but after 3 days, both approached neutral. As the amount of change in the pH of the O_2-UFB was greater than that of pure water, it was found that the wasabi greens were absorbing a large amount of components in the O_2-UFB nutrient solution. The amount of change in the electrical conductivity of each nutrient solution is shown in **Fig.9**. From the viewpoint of electrical conductivity, the O_2-UFB has a higher negative value than pure water, and it was found that the O_2-UFB wasabi greens absorbed more components. Based on these results, it was confirmed that O_2-UFB has a growth promoting effect on the wasabi greens. Moreover, since the O_2-UFB wasabi greens absorbed many components, it was thought that the O_2-UFB increased the amount of absorption of the components because the clusters of the water molecules became smaller.

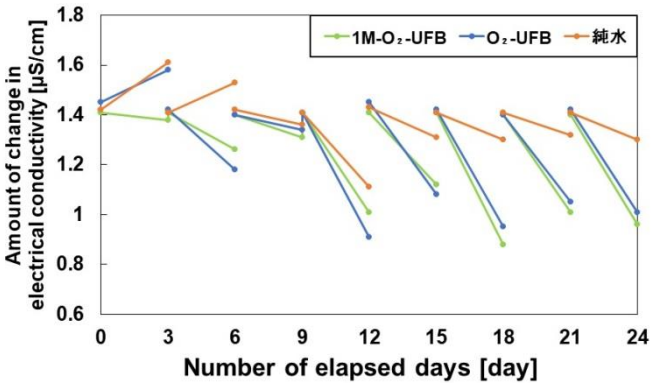

Fig.8 Change in pH of each nutrient solution

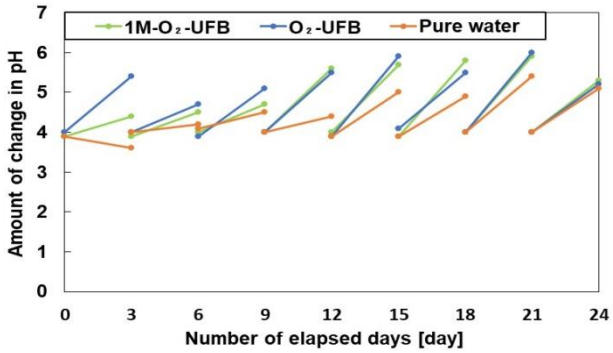

Fig.9 Change in electric conductivity of each nutrient solution

III-III Influence of O_2 -UFB on the growth of wasabi

The germination rate on the 9th day after sowing the wasabi seeds in the dark is shown in **Fig.10**. The germination rate of the wasabi was 29% for the O_2-UFB and 25% for pure water, and the germination rate for the wasabi grown with the O_2-UFB was higher than that of pure water. Based on these results, it was confirmed that O_2-UFB also has a growth promoting effect on the wasabi.

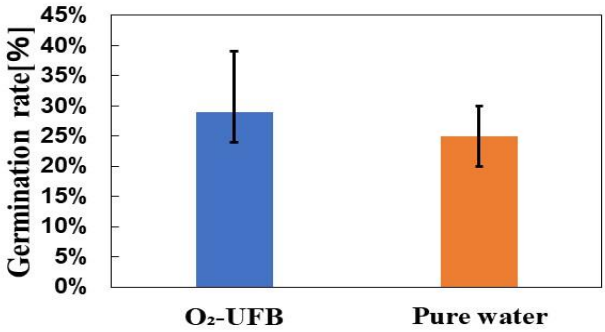

Fig.10 The germination rate of wasabi in each nutrient solution

III-IV Measurement of water absorption of wasabi seeds

The weight of the wasabi seeds before soaking in each nutrient solution was 0.0544 g for the O_2-UFB seeds and 0.0546 g for the pure water seeds. After being soaked in each nutrient solution for 90 minutes, the weight of the wasabi seeds was 0.1086 g for the seeds of the O_2-UFB and 0.1038 g for the seeds of the pure water. The difference in weight of the seeds before and after immersion in each nutrient solution was 0.0542 g for the O_2-UFB and 0.0492 g for the pure water, thus it was found that the water absorption of the O_2-UFB was higher. From this, it was thought that in the O_2-UFB, the clusters of water molecules are smaller than the pure water, and it is likely to be easily incorporated into the seeds.

III-V Confirmation of the existence of reactive oxygen in the wasabi seeds

Fig.11 shows the state of each seed immersed in the NBT solution for 4 hours. The NBT solution reacts with the active oxygen and develops a blue-black color. From **Fig. 11**, it was confirmed that there was active oxygen in the embryo because the wasabi embryo from the O_2-UFB water was dyed black. Based on this result, it was thought that the active oxygen in the O_2-UFB water acted on the plant hormone of the horseradish embryo and promoted the germination.

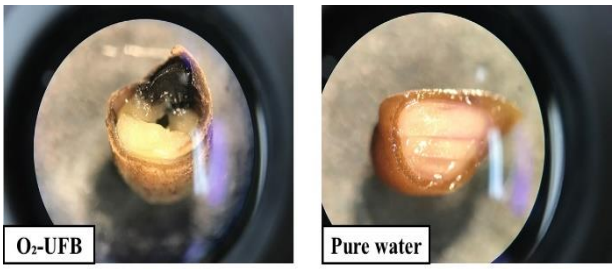

Fig.11 Cross section of seeds soaked in NBT solution

IV. CONCLUSION

In this study, in addition to examining the effect of the O_2-UFB on the wasabi growth, the influence on the growth of the wasabi greens with the same hot component of allyl isothiocyanate as wasabi was also examined. As a result, the following was determined.

- The germination rate of the wasabi greens was 89% for 1M-O_2-UFB, 88% for O_2-UFB and 78% for pure water, and it was found that the O_2-UFB has a promoting effect on the germination of the wasabi greens. In addition, it was found that the change in the size of the leaves of the wasabi greens grown in the O_2-UFB was larger than that in the pure water, and that of the O_2-UFB showed a growth promoting effect on the wasabi greens.
- Based on the amount of change in pH of each nutrient solution, it can be understood that the wasabi greens when grown with the O_2-UFB absorbs a large amount of components from the nutrient solution, and O_2-UFB has a growth promoting effect on the wasabi greens that was confirmed. In addition, from the amount of change in the electrical conductivity of each nutrient solution, it was confirmed that the wasabi greens, when grown with O_2-UFB, absorbs a large amount of components from the nutrient solution, and O_2-UFB is for the wasabi greens It turned out that a growth promotion effect was observed.
- The germination rate of the wasabi was 29% for the O_2-UFB and 25% for the pure water, and it was found that O_2-UFB was effective in promoting the germination of the wasabi. It was also found that the wasabi seeds when soaked in the O_2-UFB had a higher water absorption than the seeds soaked in the pure water.
- After soaking in the O_2-UFB and pure water for 3 days, soaking in the NBT solution for 4 hours, and observing the cross section of the wasabi seeds, it was found that the O_2-UFB wasabi embryos were dyed black, thus it was confirmed that active oxygen was present.

REFERENCES

[1] Tanaka Itsuo; “Journal of the Plant Factory Society”, Vol. 21, No. 4, **33** (2009).
[2] Hoshino Toshiaki; “Plant Protection”, Vol. 69, No. 6, **50** (2015).
[3] Koshiba Tomokazu, Kamiya Yuji, Katsumi Masayuki; “Molecular Cell Biology of Plant Hormones”, **45-136** (2006).
[4] The Nikkan Kogyo Shimbun, Inc .; “Introduction to the Fine Bubble”, The Association of the Fine Bubble Association, **33-39** (2016).
[5] Takashi Yoshida; “Latest technology of fine bubbles”, Vol 2, **164**, NTS (2014).
[6] Fernanda Yumi Ushikubo, Takuro Furukawa, Ryou Nakagawa, Masatoshi Enari, Yoshio Makino, Yoshinori Kawagoe, Takeo shiina, Seiichi Oshita ; “Colloids and Surfaces A:Physicochemical and Engineering Aspects” 361,**31-37**(2010).
[7] Tanaka Itsuo; "Environmental control and profitability evaluation in indoor hydroponic culture of wasabi using artificial light", Special production seedlings No. 20, **64-67** (2015).
[8] Shimoyama Masato, Mizota Yoko, Sueda Kae, Takahashi Shinichi; “Cultivation technology of leafy vegetables in artificial light type plant factory”, Obayashi Technical Research Institute No. 78, 1-6 (2014).

IEET Editorial Office

EEAAT - Electrical Engineering Academic Association (Thailand)
Room 409, F-Building
140 Cheum-Sampan Rd.
Nong Chok, Bangkok, Thailand 10530
Tel: +662-988-3655 ext 2216 Fax: +662-988-4026

www.journal.eeaat.or.th